UNIVERSITY OF MINNESOTA
ST. ANTHONY FALLS HYDRAULIC LABORATORY

Project Report No. 85

Unsteady Force and Cavity Characteristics for Ventilated Hydrofoils

by
J. M. WETZEL
and
K. E. FOERSTER

Prepared for
OFFICE OF NAVAL RESEARCH
Department of the Navy
Washington, D.C.
under
Contract Nonr 710(48), Task NR 062-192

June 1967
Minneapolis, Minnesota

ABSTRACT

Experimental measurements were made of the unsteady cavity and force characteristics for both forced and naturally ventilated hydrofoils of finite span submerged below a free surface. Unsteady cavity characteristics were studied for a force-ventilated wedge subjected to a sudden change in either the air flow rate to the cavity or angle of attack. Differences were observed in air entrainment rates measured for the unsteady case as compared to the corresponding instantaneous steady case. The magnitude of the differences depended on the kind of unsteadyness introduced.

Unsteady force characteristics were determined for naturally ventilated foils undergoing either a sinusoidal heaving motion or a harmonic oscillation of a trailing edge flap. The amplitude of the oscillatory lift was found to increase with increasing reduced frequency for a heaving foil, whereas the oscillatory lift was essentially constant up to reduced frequencies of 1.2 for the foil with an oscillating flap. There is limited agreement of the data with available theory.

CONTENTS

LIST OF ILLUSTRATIONS

LIST OF SYMBOLS

a - heave amplitude (measured from equilibrium position)

$\bar{a}$ - dimensionless heave amplitude, a/c

AR - aspect ratio, s/c

c - foil chord length

c_f - flap chord length

$\tilde{C}_D$ - amplitude of oscillatory drag coefficient

$\tilde{C}_L$ - amplitude of oscillatory lift coefficient

d - maximum cavity thickness

f - foil submergence, measured from foil leading edge to water surface

K - parameter

k - reduced frequency, $\omega c/V$

ℓ - cavity length

P_c - cavity pressure

P_∞ - free stream pressure

s - foil span

t - time

V - velocity

V_c - cavity volume

W - air flow rate

W_F - final weight rate of flow into cavity

W_I - initial weight rate of flow into cavity

W_o - weight rate of flow out of cavity

α - angle of attack

$\dot{\alpha}$ - $d\alpha/dt$

γ_a - specific weight of air

δ - flap angle

ρ - fluid density

σ - cavitation number, $(P_\infty - P_c)/\frac{1}{2}\rho V^2$

ϕ - phase angle

ω - angular velocity

UNSTEADY FORCE AND CAVITY CHARACTERISTICS FOR VENTILATED HYDROFOILS

I. INTRODUCTION

The force characteristics of ventilated or supercavitating hydrofoils in steady motion have been extensively investigated, both in an infinite fluid and in the presence of a free surface. Measurements of the unsteady force coefficients have also been made for various types of unsteady flow, although the data are not as complete. During an investigation at this Laboratory of the unsteady forces associated with a restrained, ventilated hydrofoil of finite span moving through a regular wave train [1]*, it was found for force-ventilated foils that problems arose relative to the behavior of cavities in unsteady flow. In an attempt to obtain additional information on the unsteady cavity characteristics, an additional series of tests was initiated to determine the cavity collapse or growth mechanism for force-ventilated foils. These tests were later extended to include the investigation of other types of unsteady flow. Thus, the tests described in this report are concerned with the following items:

1. Unsteady cavity characteristics for a force-ventilated foil at a constant angle of attack and for which the air flow rate to the cavity is suddenly changed.
2. Unsteady cavity characteristics for a force-ventilated foil with the air flow rate held constant and the angle of attack suddenly changed.
3. Unsteady force characteristics for a naturally ventilated foil of finite span at a constant angle of attack undergoing sinusoidal heaving oscillations.
4. Unsteady force characteristics for a naturally ventilated foil of finite span at a constant angle of attack with an oscillating trailing edge flap.

It should be noted that the first two items were primarily concerned with unsteady cavity characteristics for a force-ventilated foil, whereas the last two items were concerned with the unsteady force characteristics for a naturally ventilated foil. The naturally ventilated foils were utilized in the latter two items to reduce complications inherent in techniques used for force-ventilated foils.

---

*Numbers in brackets refer to the List of References on page 17.

All tests were conducted with hydrofoils of finite span in the vicinity of a free surface. Theoretical results are available for a foil undergoing heaving motions and also for a two-dimensional foil with an oscillating, trailing edge flap. Hsu [2,3] has developed a two-dimensional theory to determine the unsteady forces at zero cavitation number for a heaving and pitching foil, and also for a foil with an oscillating flap. The effect of a free surface was also taken into consideration. Song [4] improved the theory by Hsu for the trailing edge flap case. Widnall [5] attempted to account for the effects of finite span on the unsteady forces on a foil undergoing heaving oscillations, although she did not consider the effect of the free surface. Wherever possible, these theoretical results were compared with the experimental data obtained in the program.

II. EXPERIMENTAL EQUIPMENT AND PROCEDURE

The experimental work was carried out in the main towing tank, which is 9 ft wide and 6 ft deep with a useful run of about 220 ft. The water depth for all tests was maintained at 4.5 ft. The self-propelled carriage was operated at speeds up to 18 fps, the top speed being limited by the necessity of maintaining an adequate length of test run at constant velocity.

A. Change in Air Flow Rate

These studies were conducted with a 6 degree wedge foil of rectangular planform, 4 in. chord, and 10 in. span. The force-ventilation system consisted of two air supply lines leading down through the streamlined supporting strut and terminating in openings at the base of the strut. Each supply line could be controlled separately, and one supply line had a quick shut-off valve located at the point of connection to the strut. The response of the airflow into the cavity region upon closing the valve could be observed by the quantity of bubbles emerging from the strut port when the foil was stationary and submerged. Quick closure of the valve resulted in immediate stoppage of the airflow except for a few small bubbles. Cavity pressures were measured with a diaphragm-type pressure transducer mounted directly on the upper surface of the foil near the trailing edge. Such a transducer was necessary to accurately measure the instantaneous variation of cavity pressure with time. A Sanborn recorder was used for recording purposes. These observed cavity pressures were reduced to instantaneous cavitation numbers.

B. Change in Angle of Attack

These studies were also conducted with the 6 degree wedge foil of rectangular planform, 4 in. chord, and 10 in. span used for the previous tests. The foil and strut system was rotated manually about a pivot point located 20 in. above the foil by means of a long lever arm. When the system was not being rotated, it was locked firmly in place. The instantaneous angle of attack was measured with a calibrated linear potentiometer attached to the strut at the pivot point. Cavity pressure was again measured with a diaphragm-type pressure transducer. The signals were recorded with a Sanborn recorder.

C. Heaving Foils

The two foils employed for this series of tests were 6 degree wedge profiles of rectangular planform with chords of 3 and 4 in., and spans of 6 and 4 in. respectively. Both foils, and their supporting struts, were constructed of aluminum to reduce weight. The 3 in. chord foil was also fitted with circular end plates to serve as an approximation to the infinite aspect ratio case. The foils were naturally ventilated to the atmosphere by utilizing supporting struts of triangular cross-section allowing air to travel down the separated region at the rear of the strut to the separated region of the foil.

The heaving apparatus consisted of a small subcarriage traveling vertically along two fixed rods. A schematic drawing is shown in Fig. 1. The subcarriage was oscillated sinusoidally by means of a slider and eccentric pin arrangement driven by a small electric drill motor. This drive maintained positive contact, such that the free travel in either direction was less than 0.005 inch. The motions of the subcarriage were detected with a connected linear differential transformer. Frequency control was obtained with an electronic-type speed control on the drill motor providing high torque at low rpm. A two-component dynamometer was mounted on the subcarriage with its strain gage elements aligned in a vertical and horizontal direction. The sensing members of the dynamometer were pretensioned steel fibers with the load to be measured acting along the axis of the fibers. The supporting struts for the foils attached directly to the dynamometer and were kept as short as possible. The natural frequency of the dynamometer with the foil attached was between 50 and 60 cps. The maximum frequency of the heaving

oscillations was about 10 cps. The mass of the foil system and of portions of the dynamometer produced an inertial force when the apparatus was being oscillated. The magnitude of the inertial force was determined by oscillating the foil in air and measuring the resulting force. This inertial force was subtracted from the recorded lift response of the heaving foil when towed through the water, taking into consideration the phase relationship between the two forces.

D. Oscillating Flap

For the oscillating flap tests, a 6 degree wedge profile of 5 in. chord and 10 in. span with a rectangular planform was used. The foil and strut were constructed from aluminum. A sketch is shown in Fig. 2. The trailing edge flap extended over the entire span of the foil for 30 per cent of the total foil chord. The semi-circular leading edge of the flap fitted into a circular arc recess in the trailing edge of the main foil and was supported by outboard hinge pins. The hinge supports were sufficiently small to insure that they always remained in the cavity generated by the tip vortex. The hinge gap was of the order of 0.002 in. and was filled with grease. No leakage of fluid through the hinge gap was observed. The flap was actuated by a pushrod recessed in the trailing edge of the strut. The pushrod was driven by a bellows-type actuator which was attached to the top of the strut. Hydraulic power to oscillate the flap was generated by a second identical bellows driven by a small electric motor through a crankshaft and bell crank. The drive system was the same as that used for the tests conducted in the free jet water tunnel [4]. The power system was mounted separately from the foil and dynamometer unit. A flexible hydraulic line was attached to the bellows on the foil strut normal to the plane of the lift and drag forces. The hydraulic power system oscillated the flap sinusoidally up to a frequency of 5 cps. Distortions in the motion began to appear at higher frequencies due to dynamic effects associated with the hydraulic power transmission system. Motion of the flap was measured with a linear differential transformer. The extent and limits of the flap travel were adjustable. The dynamometer was the same as previously described for the heaving foil system, except that stiffer strain members were used because of the larger lift forces obtained for the relatively larger foil. When the flap was oscillated in the air, the induced response measured by the dynamometer was considered negligible compared with the actual force response obtained for the foil moving through the water.

III. DISCUSSION OF RESULTS

A. Unsteady Cavity Characteristics

Tests were undertaken to study the transient behavior of force-ventilated cavities after a sudden change in air flow rate to the cavity, or a sudden change in angle of attack of the foil.

The transient state of a cavity may be described in terms of its volume which will vary with time according to the net air inflow or outflow rate, i.e.,

$$V_c(t + \Delta t) = V_c(t) + \left(\frac{W_I - W_o}{\gamma_a}\right)\Delta t \qquad (1)$$

Where $V_c(t + \Delta t)$ = volume of cavity at time $t + \Delta t$,
$V_c(t)$ = volume of cavity at time t,
W_I = initial weight rate of flow of air into cavity,
W_o = weight rate of flow of air out of cavity,
t = time, and
γ_a = specific weight of air.

Volume changes due to cavity pressure changes were considered to be negligible during the time increment Δt. The initial air inflow rate, W_I, was a known quantity, since the cavity was force-ventilated. For a steady cavity the air outflow rate, W_o, would be equal to the inflow rate, W_I. W_I was adjusted to yield a certain cavitation number, σ, at a given angle of attack, α. Thus W_o, in turn, was also a function of σ and α. For an unsteady cavity, the instantaneous air outflow rate corresponding to instantaneous σ or α was assumed to be the same as that found for steady flow conditions at the same σ or α. Thus a quasi-steady flow process could be formed by making σ or α functions of time. To estimate the volume of the cavity it was assumed that the cavity could be approximated by an elliptical cylinder having the cavity length, ℓ, as the major axis, the maximum cavity thickness, d, as the minor axis, and the foil span, s, as the cylinder length. In the towing tank experiments, the cavity thickness was not readily measured. However, measurements [6] made in a free-jet tunnel showed that

$$\frac{d}{\ell} \approx 2\sigma \tag{2}$$

for a foil of aspect ratio 2.5. Thus the cavity volume was approximated by

$$V_c \approx \frac{\pi}{2} s\sigma\ell^2 \tag{3}$$

For a given foil at a fixed angle of attack and submergence, it was assumed that the cavity length may be expressed as

$$\ell = \frac{n}{\sigma} \tag{4}$$

Substituting Eq. (4) into Eq. (3), it is seen that the cavity volume is inversely proportional to the cavitation number, i.e.,

$$V_c \approx \frac{K}{\sigma} \tag{5}$$

where $K = \frac{\pi}{2}sn^2$, $n = \phi(\alpha,f)$, and f is the foil submergence.

With the above assumptions, it is possible to express the cavity volume as a function of the cavitation number only if all other variables are held fixed. The results of cavity length measurements for steady state cavities are shown in Fig. 3 in dimensionless form by the solid line; the broken line will be discussed later. These data were taken at various angles of attack and a submergence, f, of one chord. Cavity length was measured as the distance from the leading edge of the foil to the estimated tail of the cavity.

The air flow rate as a function of the cavitation number is shown in Figs. 4 and 5 for the particular foil employed in these tests at various velocities and angles of attack. These curves are typical air entrainment curves for ventilated cavities and were obtained by fairing lines through experimental data not shown in these figures. For a given angle of attack and velocity, a minimum cavitation number exists which is apparently independent of the air flow rate. For lower air flow rates, the cavitation number is essentially proportional to the ventilation rate. This latter region is known to be associated with the existence of a rather strong reentrant jet, and in the former region the reentrant jet is difficult to distinguish. The quasi-steady flow calculation procedure for a given foil and a transient cavity

associated with either a change in the angle of attack or the air flow rate involved the following steps:

1. The volume of the cavity was determined from the cavitation number, σ_1, at the time the cavity pressure began to change.
2. A preliminary estimate of a cavitation number, σ_2, was made after a convenient incremental time period, Δt, usually taken as 0.5 sec. (Smaller time increments were also tried, but the effect on the results did not warrant the additional effort required in calculation.)
3. The air outflow rate during the time, Δt, was estimated by averaging the air flow rates taken from Fig. 5 for σ_1 and σ_2 and corresponding α_1 and α_2 if the angle of attack was changing during this time period.
4. From the average air outflow rate and the air inflow rate, if there was one, a change in cavity volume over the incremental time period was calculated.
5. The new cavity volume as determined from Eq. (1) corresponded to a cavitation number which should be equal to the value of σ_2 estimated in Step 2. If this was not the case, the procedure was repeated with a second estimate of σ_2.

1. Unsteady Cavity Characteristics Associated with Sudden Variation in Air Flow Rate

The cavity pressure in force-ventilated cavities was investigated for the case of a sudden reduction in air flow to the cavity, since this process could be readily achieved with reasonable certainty with the test apparatus. The reverse process of a sudden increase in air flow to the cavity was difficult to obtain because of the time element required to establish a given steady flow into the cavity from the air supply tank. In addition, the time required to establish a steady cavity for the initial air supply rate would have taken up too much of the test run to permit observation of a cavity change after an increase in air flow was initiated. Therefore, no attempt was made to obtain quantitative results for the case of a sudden increase in the air flow rate.

The time history of cavity collapse (or the change in cavity pressure and thus cavitation number) for the case of complete shutoff of the inflow air supply is shown in Fig. 6 for several towing velocities. For each test

run the same high rate of airflow (W_I = 10.2 x 10^{-3} lbs/sec) was supplied to the cavity during the acceleration portion of the run. Because of the limited length of the towing tank, the cavitation number corresponding to the air supply rate as shown in Fig. 4 was not attained. The cavity that was obtained at the time of air shutoff was in the transition region from a reentrant jet to a non-reentrant jet type of cavity in each case, as again can be seen by reference to Fig. 4 for the cavitation numbers at $t = 0$ in Fig. 6a. With the same air supply rate the variation in velocity yielded different cavitation numbers and, consequently, varying cavity lengths. Examination of the experimental data plotted in Fig. 6a shows that the rate of increase of the cavitation number is about the same up to σ values of about 0.12 for each velocity except the lowest. Thereafter, σ increases more rapidly with time. The calculated values shown by the solid lines agree with the actual values only during the initial stages of cavity collapse and the method is wholly inadequate to describe the cavity change for the larger σ's. In general, it appears that the change in cavity pressure or cavitation number can be predicted with some success for cavities in which a strong reentrant jet does not exist. For cavities with a strong reentrant jet, the air entrainment mechanism may be considerably different than that for steady cavities.

Additional data for collapsing cavities are shown in Fig. 6b. The data taken at 18 fps are a continuation of the tests shown in Fig. 6a. At 18 fps only a relatively short record of the cavity pressure could be obtained due to limitations in the length of the test run. This run is also very similar to that taken at 16 fps, the two runs achieving about the same cavitation number before air supply shutoff. The data taken at 12 fps (triangles) are similar to the data in Fig. 6a at 12 fps except that the initial air supply rate to form the cavity during the acceleration run is about half as large. Again both runs achieve about the same cavitation number at the time the air supply is shut off and consequently have the same cavity decay characteristics. The other set of data in Fig. 6b for a velocity of 12 fps (circles) illustrates a slow cavity change when a residual air supply (W_F = 2.45 x 10^{-3} lbs/sec) is maintained after a sudden reduction of the initial high air supply rate (W_I = 9.24 x 10^{-3} lbs/sec). During the first seven seconds, σ has changed from 0.103 to 0.125, whereas extrapolation of the curve from Fig. 4 for the residual air supply rate W_F indicates a terminal σ of 0.24. The quasi-steady calculations fit the actual change quite well over the limited range of cavitation

numbers for which data are available. The quasi-steady procedure for calculating cavity change as outlined in the preceding section neglected certain factors or conditions that could have an effect upon the calculated results:

1. Cavity volume occupied by the reentrant jet was not taken into consideration.
2. The entrainment of air by the reentrant jet may be different in a transient cavity from that in a steady state cavity.
3. The volume of short cavities is poorly approximated by an elliptical cylinder.
4. The relationship between the cavity length and cavitation number may differ between steady and transient cavities.

Item 1 may be the reason that the calculations agree with the actual results during the initial change of the cavity. The cavities at the time of air supply shutoff were of the non-reentrant jet type or at least in the transition region. The establishment of the reentrant jet after the shutoff of the air supply would mean an additional loss of cavity volume other than by a reduction in length. The possibility that the entrainment process or cavity characteristics are different for transient cavities from those of steady cavities would be indicated if for identical cavitation numbers in each case, the cavity length would be different. This was found to be the case when high-speed motion pictures of collapsing cavities were correlated with the recorded instantaneous cavity pressures. The results are shown by the broken line in Fig. 3. The transient cavities are slightly longer for a given cavitation number than steady state cavities, although it must be admitted that accurate measurements of the cavity length are difficult to obtain. The calculations were revised by basing the cavity volume on the σ vs ℓ relationship for a transient cavity. However, the improvement of the revised predictions was small. Calculated values shown in Fig. 6 are based on the revised values of the cavity volume.

2. Unsteady Cavity Characteristics Associated with Sudden Variation in Angle of Attack

A change in angle of attack represents another method of creating a transient cavity. If the air supply to a force-ventilated cavity is held constant, an increase in angle of attack will cause the cavity to shorten, and a decrease in angle of attack will cause it to lengthen. This can be readily inferred from Fig. 5. The angle of attack was varied between 12 and

19 degrees. This range was selected to yield a large change in cavitation number and still insure that the foil would ventilate readily at the lower angle of attack for a velocity of 12 fps. All experiments were conducted with a constant air supply rate of 0.00460 lbs/sec, which resulted in a rather long non-reentrant jet cavity at 12 degrees and a short reentrant jet cavity at 19 degrees. A towing velocity of 12 fps was selected so that the change in cavity pressure could be recorded over the longest possible time. The angle of attack was changed at either a fast rate ($\dot{\alpha} = \frac{d\alpha}{dt}$) such that the total change of 7 degrees took less than one second, or a relatively slow rate such that the duration of the change extended over most of the test run.

Figure 7 shows the changes in cavity pressure, reduced in terms of the cavitation number, as the angle of attack was increased from 12 to 19 degrees with the air flow rate held constant. In Fig. 7a, the total angle change occurred in about 6.4 seconds. The cavitation number for α = 19 degrees for the given flow rate was about 0.22. Therefore, the cavity did not attain its terminal value for this run. The quasi-steady calculations previously described and shown as filled symbols indicate a somewhat faster change of cavitation number than actually obtained. In Fig. 7b, the total angle change required only about 0.23 seconds. At the end of this time, σ was about 0.17, whereas it again should have been 0.22. The measured decay characteristics are also seen to be different than the calculated values.

Two sets of data are shown in Figs. 8a and b for the case when the angle was decreased from 19 to 12 degrees. The variation of cavitation number with time is shown with circular symbols, and the variation of cavitation number with angle of attack is shown with triangular symbols. As simultaneous records were taken of the instantaneous angle of attack and cavity pressure, cavitation numbers were calculated for a number of angles; these values are shown as the open triangles. The broken line represents the relationship between cavitation number and angle of attack obtained by cross-plotting data from Fig. 5 for the given air flow rate. It is immediately seen that a large discrepancy exists between the data and the steady values shown by the broken line. Better agreement was found with the calculations based on the quasi-steady process previously described and shown as filled symbols. Data are shown in Fig. 8c for fast angle changes, the total angle change occurring in about 0.3 and 0.09 seconds for the two conditions shown. A rather rapid decrease in σ was noted over these short time intervals, followed by a much

slower decrease with time after the final angle of attack (12 degrees) was attained.

B. Unsteady Forces for Heaving Foil

Experimental data for the unsteady lift coefficient due to heaving motion for the aspect ratio 2 foil are plotted in Fig. 9. The total lift on the oscillating foil consisted of the steady lift at equilibrium conditions and the oscillatory lift due to the heaving motion. The ordinate is the amplitude of the oscillatory lift reduced to a lift coefficient divided by the amplitude of the heaving motion, made non-dimensional by the foil chord. The abscissa is the reduced frequency based on the foil chord. These data were taken at a one-chord submergence and the angle of attack was maintained at 14 degrees in an attempt to insure the existence of a cavity for all frequencies of oscillation. Two heave amplitudes, as indicated by the open and filled symbols, were used. Theoretical results from Hsu for both a two-dimensional foil in an infinite fluid and at a one-chord submergence are shown, as well as Widnall's result for an aspect ratio 1 foil in an infinite fluid. The theoretical amplitude of the oscillatory lift increases quite rapidly with increased values of the reduced frequency. The experimental data generally fall between Hsu's and Widnall's theoretical results. It can also be noted that the lift coefficient varies linearly with amplitude of motion, as the data for both amplitudes agree within the experimental scatter.

One series of tests was conducted with end plates attached to the foil in an effort to reduce the effects of finite span. These data are shown in Fig. 9 as flagged symbols. The data are essentially the same as the data taken without end plates, indicating that either the end plates were not of sufficient size or that the effect of aspect ratio is small for a heaving foil. However, Widnall's theory implies that decreasing the aspect ratio reduces the amplitude of the oscillatory lift considerably.

The phase angle of the oscillatory lift for the aspect ratio 2 foil is plotted in Fig. 10. The phase angle is defined as the number of degrees that the maximum lift lagged the maximum upward heaving motion of the foil. Here again the agreement with theory is generally good, although at the higher values of the reduced frequencies, some discrepancy is noted. The accuracy of the data for phase relationships is less than that for force amplitude,

and thus some of the discrepancy observed particularly at the higher frequencies may be related to experimental errors.

Some tests were also conducted with an aspect ratio 1 foil so that a more direct comparison could be made with the theoretical results calculated by Widnall. The results of these tests are plotted in Fig. 11 for one amplitude of heaving oscillation. The data again fall between the theoretical curves for foils with an aspect ratio of infinity and one. In fact, by a direct comparison of Fig. 9 and Fig. 11, it can be seen that the experimental data for the aspect ratio 1 and 2 foils are generally in close agreement.

The cavitation number indicated in these figures has been calculated from the mean submergence of the foil and the velocity. It was assumed that cavity pressure was atmospheric, as the foil was ventilated to the atmosphere. The cavitation number for the two foils of different chord lengths is thus slightly different for the same velocity, as the submergence ratio, f/c, of both foils was held constant.

The relatively large angle of attack (14 degrees) used for the tests was selected so that a stable cavity would exist during the test run. However, it was found that even with this large angle of attack, for some conditions the cavity was washed off the foil. This behavior was further investigated by varying the angle of attack, frequency of oscillation, and towing velocity. The results are shown in Fig. 12 for the aspect ratio 2 foil at a one-chord submergence and three angles of attack. As an example, consider the angle and velocity constant, and the heaving frequency being gradually increased from some initially low value. For any frequency to the left of the lines for a given angle of attack, a full cavity was maintained throughout the test run. As the frequency was increased, a value was reached at which the full cavity was lost after about 30 cycles of heaving. These values are shown by the broken line. The solid line indicates values of the frequency at which a rapid loss of the cavity occurred in less than 5 cycles of heaving. Thus, any frequencies to the right of the solid line were considered to result in cavity wash-off. As expected, cavity wash-off occurred at higher frequencies for the larger angles of attack. Some computations were also made in an effort to predict the frequency at which wash-off may take place. In earlier tests described in Reference [7], experimental data were taken concerning the minimum angle of attack for which a stable cavity would exist in

steady flow for this particular foil. The instantaneous angle of attack was then calculated from the frequency of heaving oscillation. The predicted values based on steady flow tests are shown as filled symbols in Fig. 12. Reasonable agreement with the measured values in unsteady flow can be noted. It should also be mentioned that once the cavity had been washed off the foil, it did not reform during the test run.

C. Unsteady Forces for Foil with Oscillating Flap

Experimental data for the oscillatory lift coefficient as a function of reduced frequency are shown in Fig. 13. Here $2\tilde{C}_L$ is the double amplitude of the oscillatory lift reduced to coefficient form, and δ is the total deflection angle of the oscillating flap. The reduced frequency is again based on the full chord length of the foil. Data are plotted for submergence ratios of one, one-half, and zero --the latter for only one towing velocity. In Fig. 13a, for the lowest towing velocity used in the tests, it can be seen that for $f/c = 1$ the lift coefficient increased considerably with reduced frequency. As the submergence of the foil was decreased, the dependence on reduced frequency diminished, and the lift coefficient was essentially constant. For the other towing velocities, the oscillatory lift coefficient was relatively independent of reduced frequency for the range covered. It can also be noted that, in general, the effect of decreasing the submergence was also to decrease the amplitude of the lift oscillation.

Several tests were conducted to determine the influence of the amplitude of flap oscillation. Total flap deflections of 10 and 20 degrees were used. These relatively large values were selected so that the oscillatory lift would be sufficiently large to permit accurate measurement. The data in Fig. 13 indicate that the amplitude of the lift varies linearly with flap amplitude, even for these large flap deflections.

As previously mentioned, theory for a ventilated hydrofoil of finite span with an oscillating flap is not available. Therefore, reference is made to theory for a two-dimensional foil at zero cavitation number by Song [4]. This theory also considered the effect of free surfaces for a foil placed in a vertical, free jet. Results for a flat plate with a 30 per cent flap in both symmetrical and non-symmetrical jets were presented. For a symmetric jet, i.e., for the case where the foil is located on the jet centerline, the effect of the free surfaces is essentially negligible for half jet widths

greater than five chord lengths. As the jet width decreases, the amplitude of the lift is also decreased. The phase angle of the lift coefficient changed very little with jet width.

For non-symmetrical jets with a large depth of fluid on the pressure side of the foil, the free surface effect became significant for foil submergences of less than one chord. Experimental data taken in the free-jet water tunnel for a three-chord submergence of the pressure side indicated little difference in the amplitude of oscillatory lift for suction side submergences of one and one-half chord submergences. An increase in lift was noted as the suction side submergence was reduced to zero. The experimental data for phase angle of the oscillating lift again was essentially independent of the location of the free surfaces.

The experimental data taken in the towing tank indicated an opposite effect of the free surface on the amplitude of the oscillatory lift than that predicted and found experimentally in the free jet water tunnel. This difference may be associated with the non-zero cavitation number at which the tests were run in the towing tank.

Experimental data for the variation of the oscillatory drag as a function of reduced frequency are shown in Fig. 14. It should be noted that the drag data have been grouped with regard to submergence rather than velocity as in the previous case for the oscillatory lift. As the strut drag was not subtracted from the total measured drag, it was felt more informative to use submergence rather than velocity as the basis of comparison. The solid symbols in Fig. 14a represent a 10 degree flap deflection and the open symbols represent a 20 degree flap deflection. With the exception of the data for a velocity of 10 fps, the amplitude of the oscillatory drag is essentially independent of reduced frequency. The previously discussed data for the lift coefficient indicated that the lift was a linear function of the amplitude of flap deflection. In the case of drag, as seen in Fig. 14a, an increase in the flap deflection amplitude resulted in an increase in drag. This increase is at least partially associated with the increase in strut drag due to the larger run-up of the water on the sides of the strut. Visual observations of the flow pattern about the strut revealed that such behavior was actually taking place. The limited data, taken at a zero submergence, of course, are not influenced by strut drag.

The phase lead for the oscillatory lift for the three submergence ratios is shown in Fig. 15. The phase angle was defined as the number of degrees that the maximum lift leads the maximum deflection of the flap. Considerable scatter of the experimental data existed; however, more scatter is inherent in measuring phase angles in unsteady flow phenomena. In Fig. 15a, no significant trend can be noted with variation of the amplitude of flap deflection. The solid line drawn in Fig. 15a is based on the theory by Song for a two-dimensional foil in an infinite fluid at zero cavitation number. As the numerical computations are extremely lengthy, calculations were not carried out for other conditions. The experimental data for the small aspect ratio foil agree well with the two-dimensional theoretical result, indicating that effects of finite span may be minor in determining phase angles. In comparing data for the various submergence ratios, the phase angle for a given frequency apparently is not greatly affected by the foil submergence. At the higher reduced frequency, the phase angle may increase slightly as the submergence is decreased.

IV. CONCLUSIONS

1. When the air-flow rate to a force-ventilated foil at a constant angle of attack was suddenly shut off, it was found that the measured change in cavity pressure differed significantly from the instantaneous cavity pressure based on steady state tests, particularly for shorter cavities. It thus appears that the steady and unsteady air entrainment rates may be significantly different for short cavities in which the reentrant jet is the primary mechanism of air entrainment. For the longer cavities, which have other modes of air entrainment, better agreement was obtained.

2. If the angle of attack of a force-ventilated foil supplied with a constant air flow rate was suddenly increased, the cavity pressure changed somewhat more slowly than that predicted on the basis of steady flow measurements. In this case, the cavity shortened with increase in angle of attack. If the angle of attack was suddenly decreased (cavity length increased), the relationship between the instantaneous

cavitation number and angle of attack was considerably different from that determined by steady flow tests, the instantaneous cavity being shorter than expected.

3. For a naturally ventilated hydrofoil undergoing sinusoidal heaving motions, the following may be stated:

   (a) The amplitude of the oscillatory lift increased with increasing reduced frequency and was essentially linearly related to the amplitude of heave. The experimental data for wedge profiles with aspect ratios 1 and 2 were slightly below theoretical results for a two-dimensional foil at zero cavitation number. Agreement between theory and experiment was improved through consideration of the free surface effects. Theoretical results for an aspect ratio 1 foil in an infinite fluid were lower than the experimental data.

   (b) Addition of end plates to the heaving foil did not influence the oscillatory force characteristics. Also, no significant differences in data were observed for foils of aspect ratios 1 and 2.

   (c) The oscillatory lift lagged the heaving motion by an angle that decreased with increasing reduced frequency. Variation of heave amplitude did not result in any changes in the phase relationships.

4. For a naturally ventilated, restrained foil of finite span with an oscillating trailing edge flap, the following may be stated:

   (a) The amplitude of the oscillatory lift for a given flap deflection was essentially constant for reduced frequencies (based on the foil chord) less than 1.2, except at a low velocity. At low velocities the oscillatory lift increased with increasing reduced frequency.

   (b) The amplitude of the oscillatory lift was linearly related to the amplitude of flap oscillation.

   (c) As the foil approached the free surface, the amplitude of the oscillatory lift decreased for a given reduced frequency.

   (d) The oscillatory lift led the flap deflection by an angle that increased as the reduced frequency was increased. The measured phase angles compared favorably with theoretical results for a two-dimensional foil at zero cavitation number in an infinite fluid.

LIST OF REFERENCES

[1] Wetzel, J. M. and Maxwell, W. H. C., Force Characteristics of Flapped, Ventilated Foils in Smooth and Rough Water, University of Minnesota, St. Anthony Falls Hydraulic Laboratory Project Report No. 66, January 1963.

[2] Hsu, C. C., Fully Cavitating Hydrofoils in Non-Steady Motion under a Free-Surface, Hydronautics, Inc. Technical Report 119-5, August 1963.

[3] Hsu, C. C., Non-Steady Hydrodynamic Characteristics of a Supercavitating Hydrofoil Under a Free-Surface, Hydronautics, Inc. Technical Report 463-2, April 1964.

[4] Song, C. S., Supercavitating Flat-Plate with an Oscillating Flap At Zero Cavitation Number, University of Minnesota, St. Anthony Falls Hydraulic Laboratory Technical Paper No. 52, Series B, November 1965.

[5] Widnall, Shelia Evans, "Unsteady Loads on Supercavitating Hydrofoils of Finite Span," Journal of Ship Research, Vol. 10, No. 2, June 1966, pp. 107-118.

[6] Schiebe, F. R. and Wetzel, J. M., Further Studies of Ventilated Cavities on Submerged Bodies, University of Minnesota, St. Anthony Falls Hydraulic Laboratory Project Report No. 72, October 1964.

[7] Wetzel, J. M. and Foerster, K. E., Force Characteristics of Restrained, Naturally Ventilated Hydrofoils in Regular Waves, University of Minnesota, St. Anthony Falls Hydraulic Laboratory Project Report No. 68, March 1965.

Summary Report of ONR Contract Nonr 710(48), Task NR 062-192

The investigations carried out under this contract are fully described in the following two project reports published by the University of Minnesota, St. Anthony Falls Hydraulic Laboratory:

1. F. R. Schiebe and J. M. Wetzel, Further Studies of Ventilated Cavities, Project Report No. 72, October 1964.
2. J. M. Wetzel and K. E. Foerster, Unsteady Force and Cavity Characteristics for Ventilated Hydrofoils, Project Report No. 85, June 1967.

Project Report No. 72 describes experimental studies that were conducted to determine the air requirements of ventilated cavities on finite-span hydrofoils and other submerged bodies near a free surface. These studies were restricted to steady state conditions.

The studies were later extended to hydrofoils operating under transient cavity characteristics and are reported in Project Report No. 85. The work included force measurements of naturally ventilated foils undergoing either sinusoidal heaving motion or a harmonic oscillation of a trailing edge flap, and unsteady cavity measurements on a force-ventilated wedge subjected to a sudden change in either the air flow rate to the cavity or angle of attack.

F I G U R E S

(1 through 15)

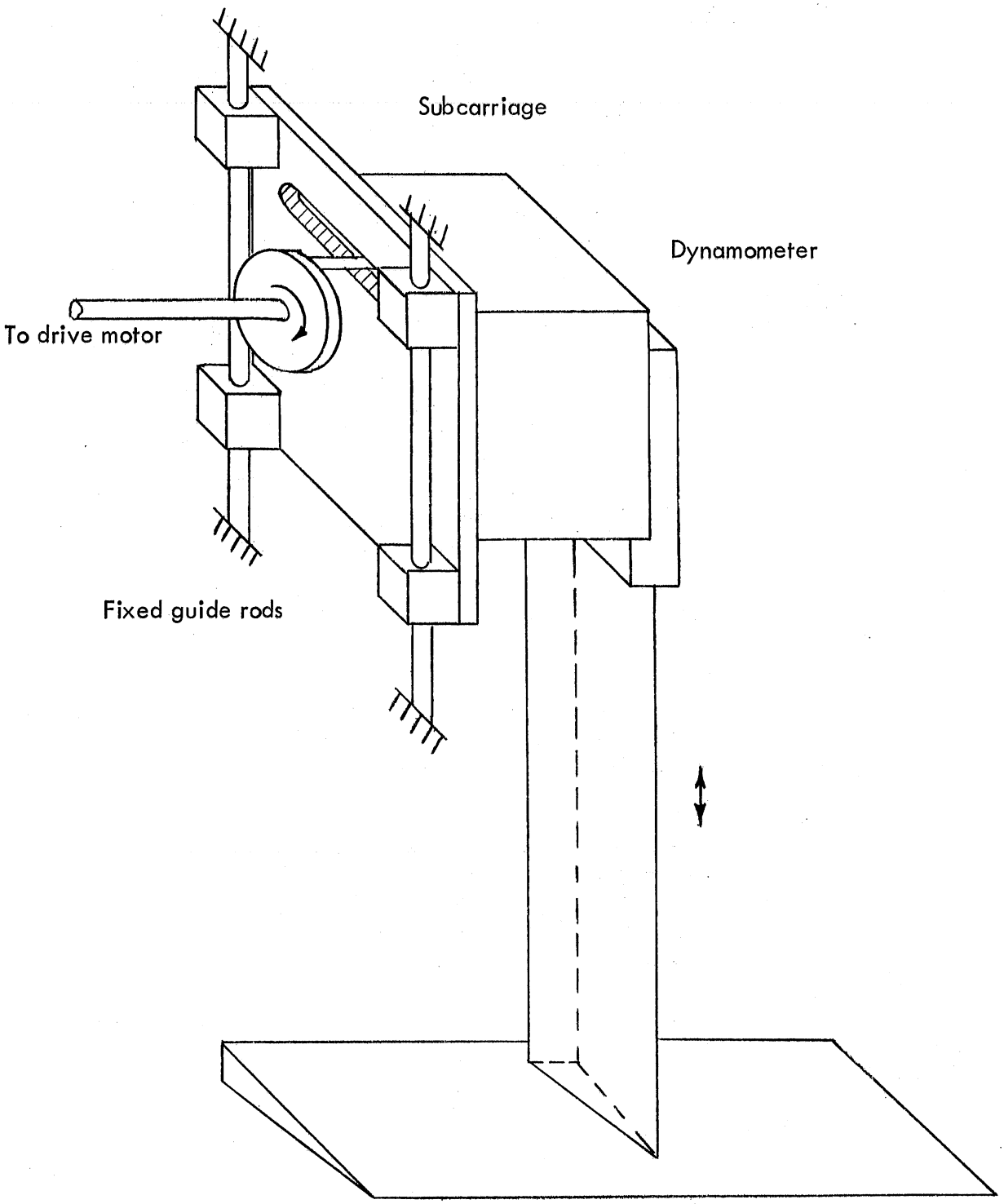

Fig. 1 - Sketch of Apparatus for Heaving Foil

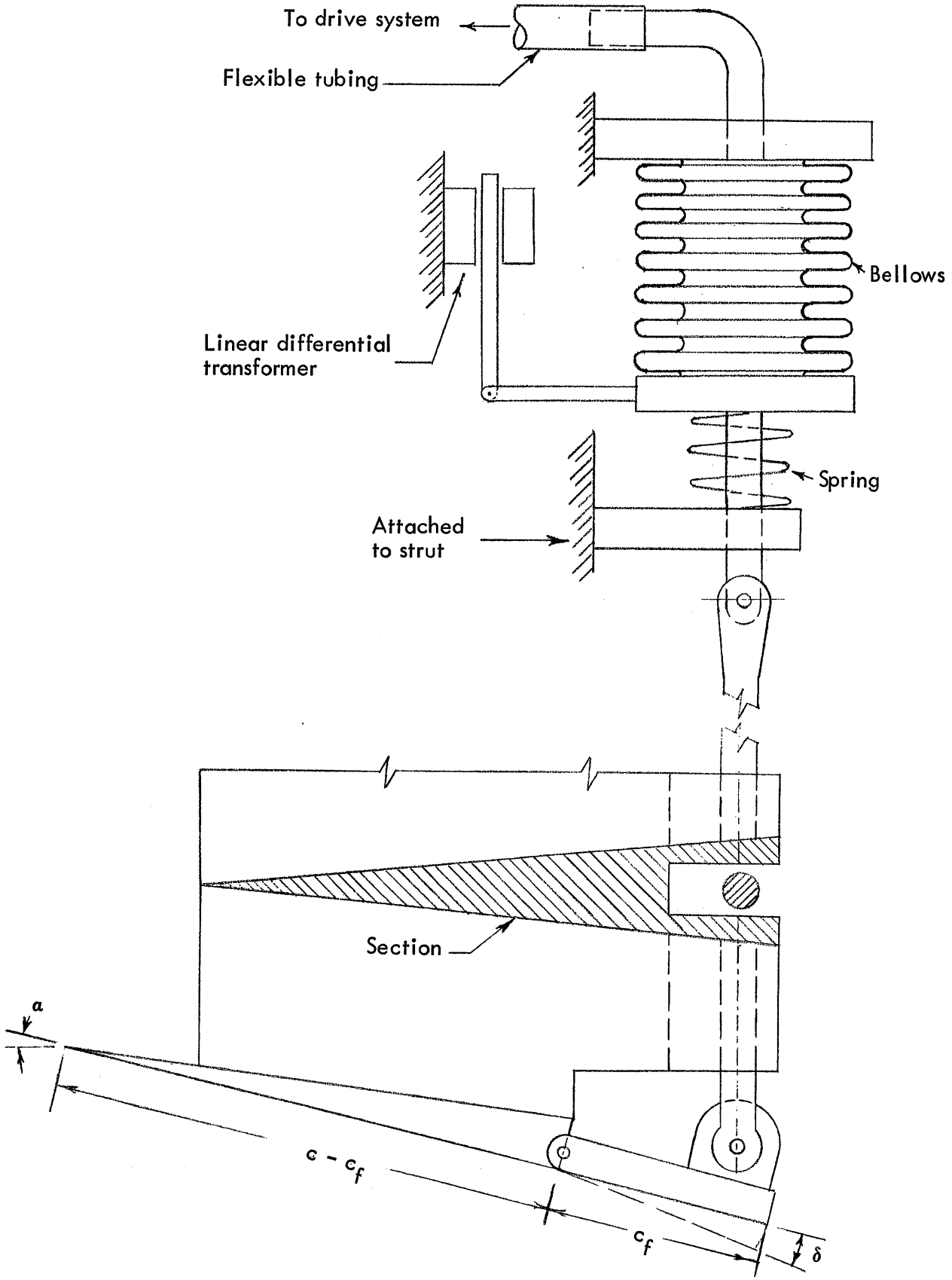

Fig. 2 - Sketch of Apparatus for Oscillating Flap Foil

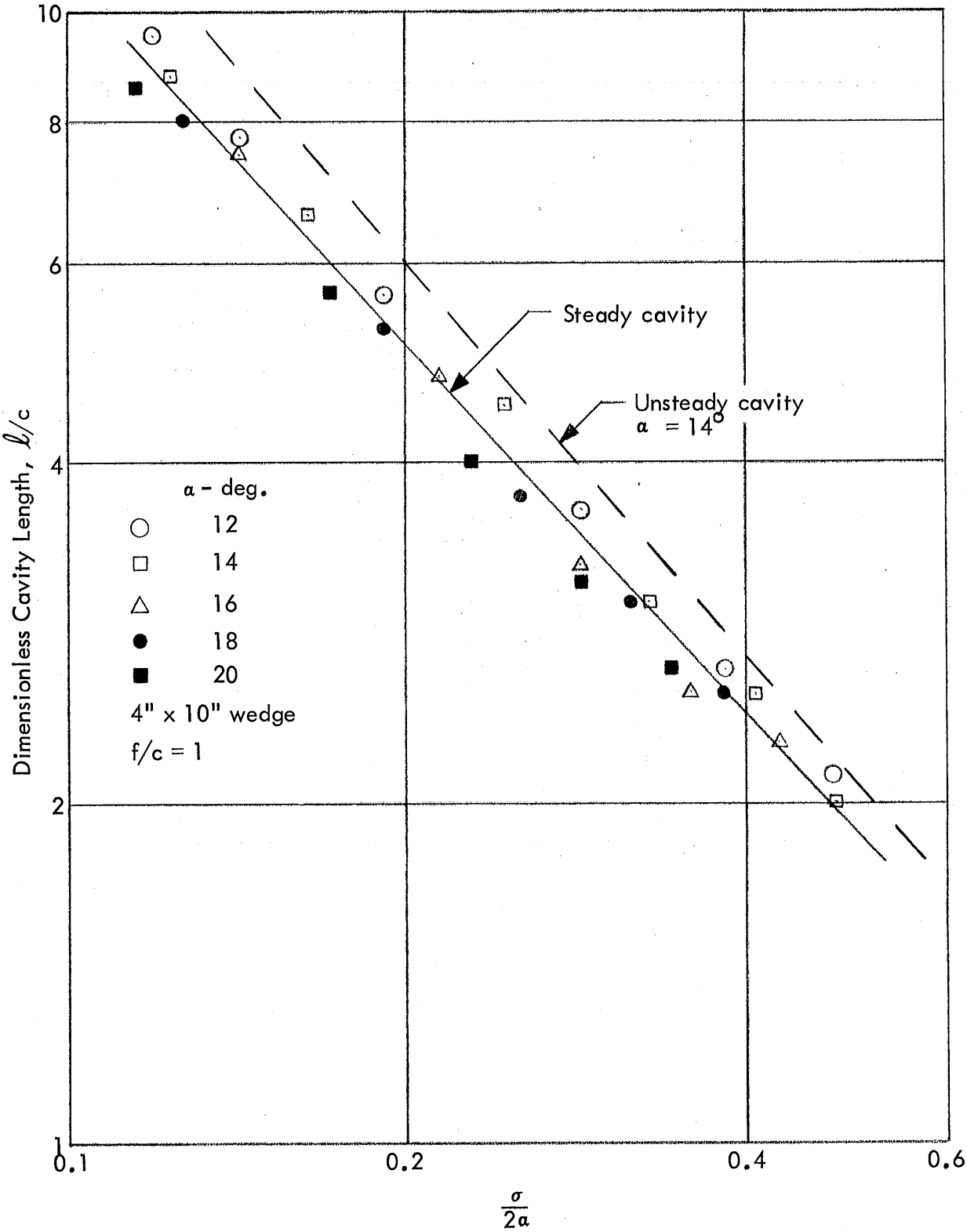

Fig. 3 - Cavity Lengths for Steady and Unsteady Cavities

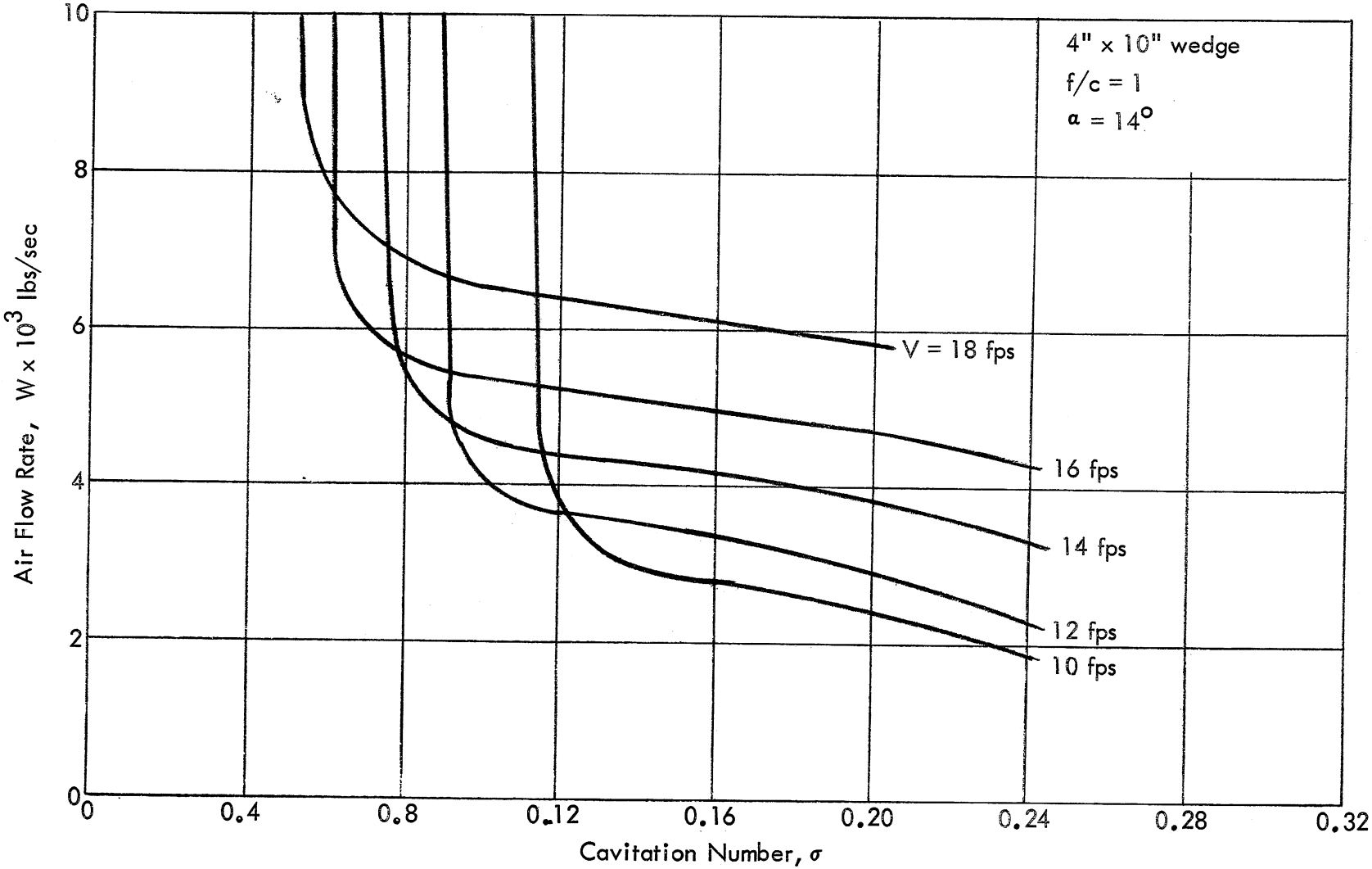

Fig. 4 - Steady Air Entrainment Rates for Various Velocities - Constant Angle of Attack

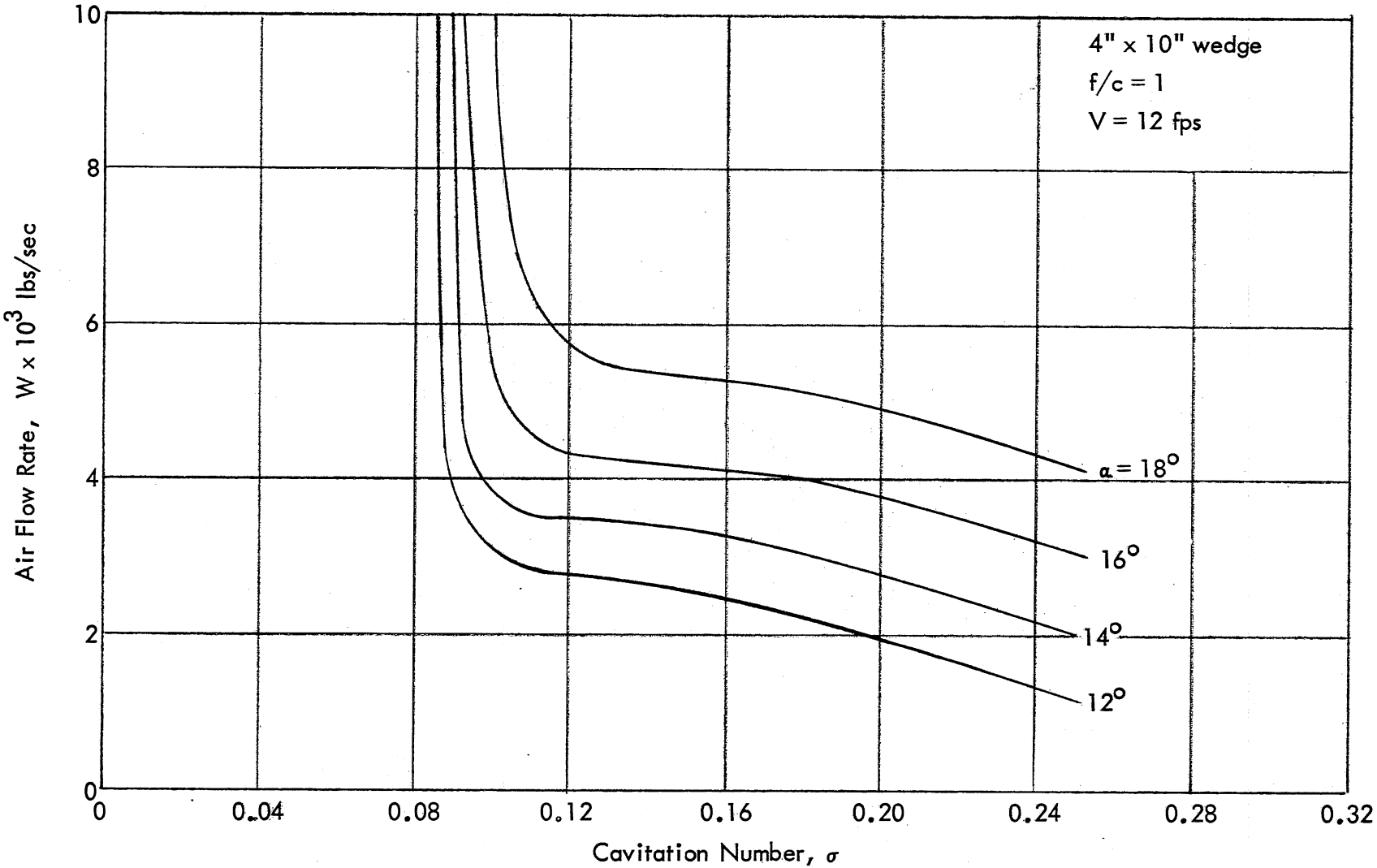

Fig. 5 - Steady Air Entrainment Rates for Various Angles of Attack - Constant Velocity

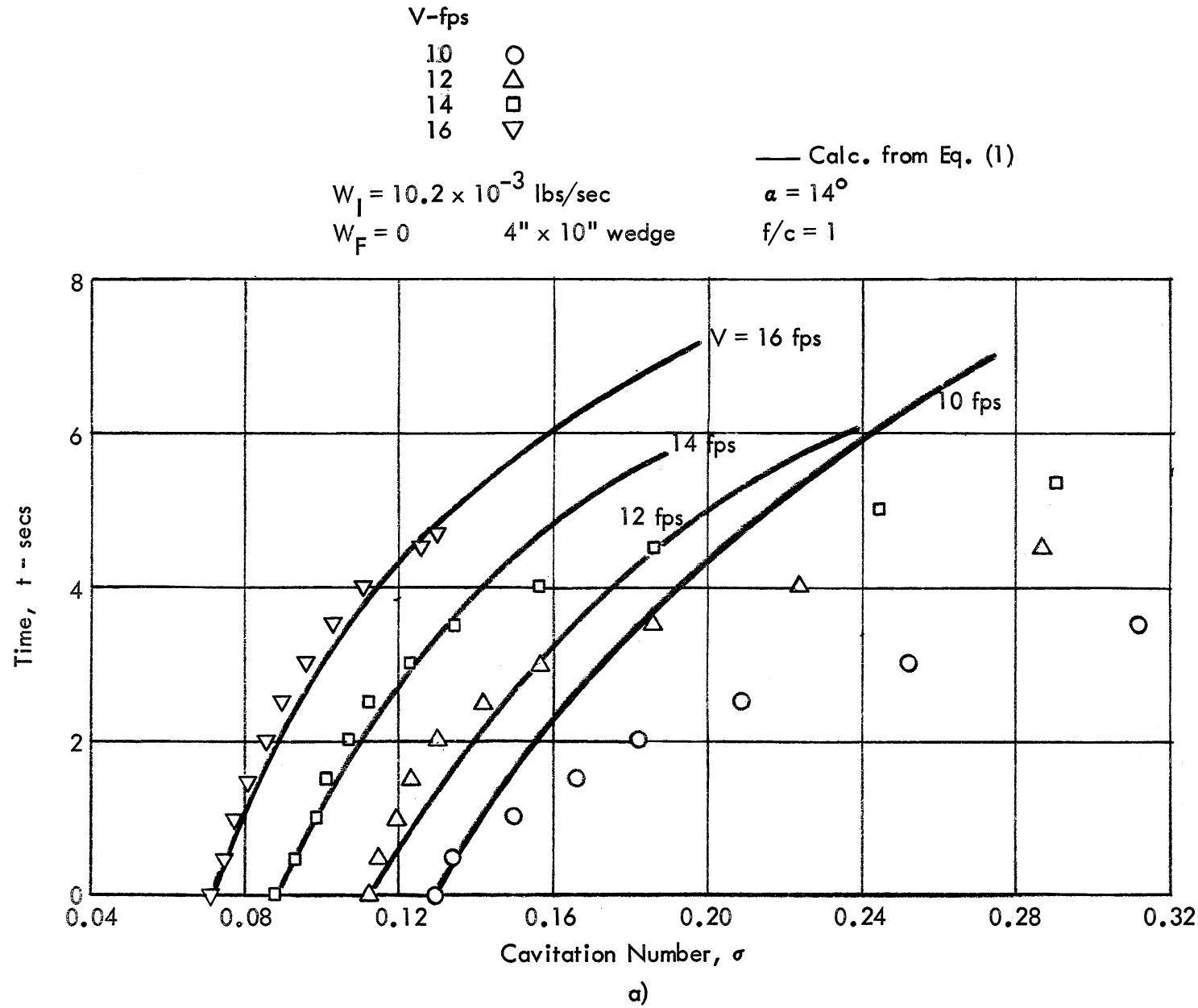

a)

Fig. 6 - Instantaneous Cavitation Numbers for Collapsing Cavities

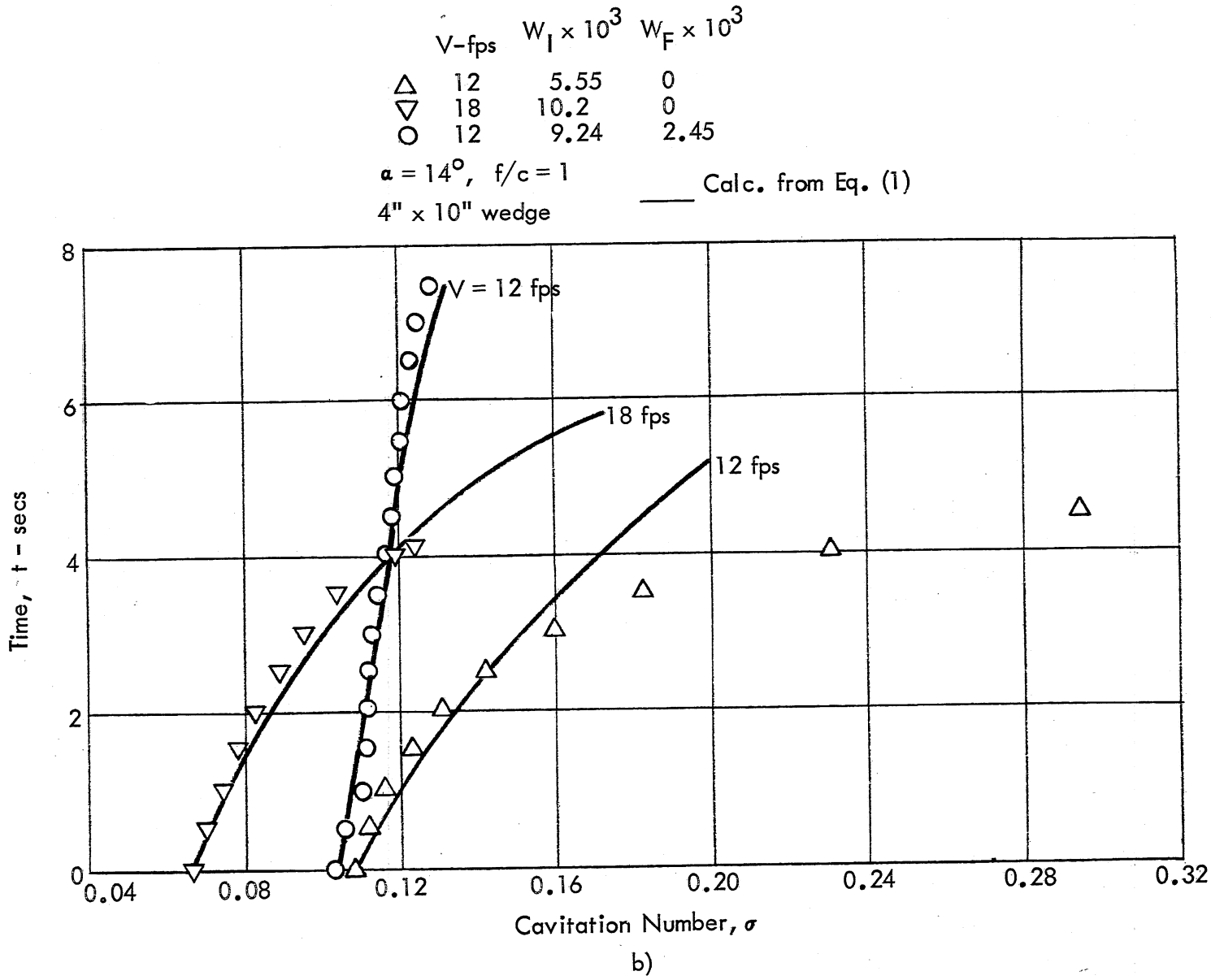

b)

Fig. 6 (contd.) - Instantaneous Cavitation Numbers for Collapsing Cavities

Open Symbols - measured
Filled Symbols - calculated
$W = 4.60 \times 10^{-3}$ lbs/sec
f/c = 1, V = 12 fps
4" x 10" wedge

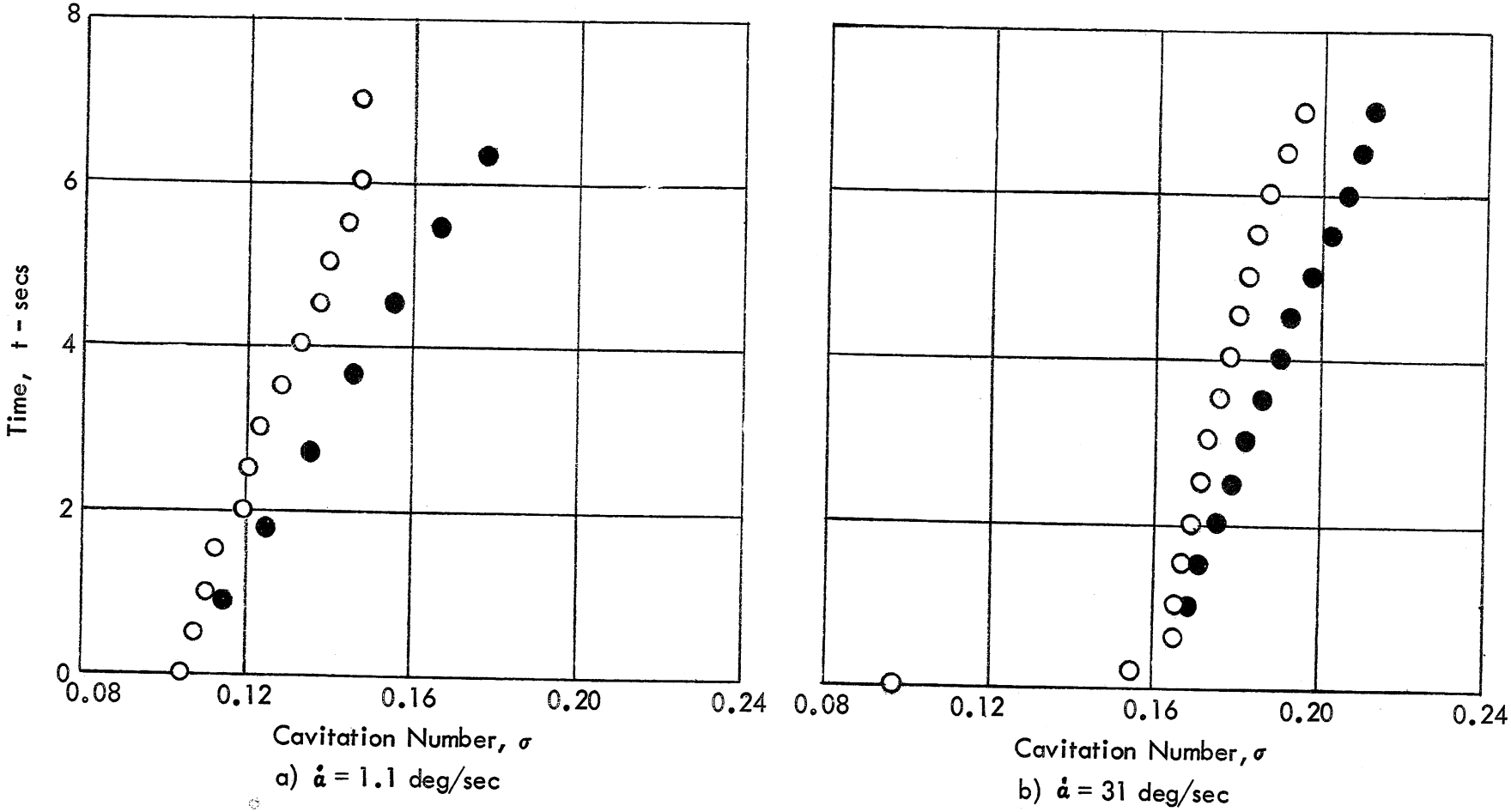

Fig. 7 - Change in Cavitation Number with Increasing Angle of Attack, 12° to 19°

Open Symbols - measured

Filled Symbols - calculated

$W_l = 4.6 \times 10^{-3}$ lbs/sec

f/c = 1, V = 12 fps

4" x 10" wedge

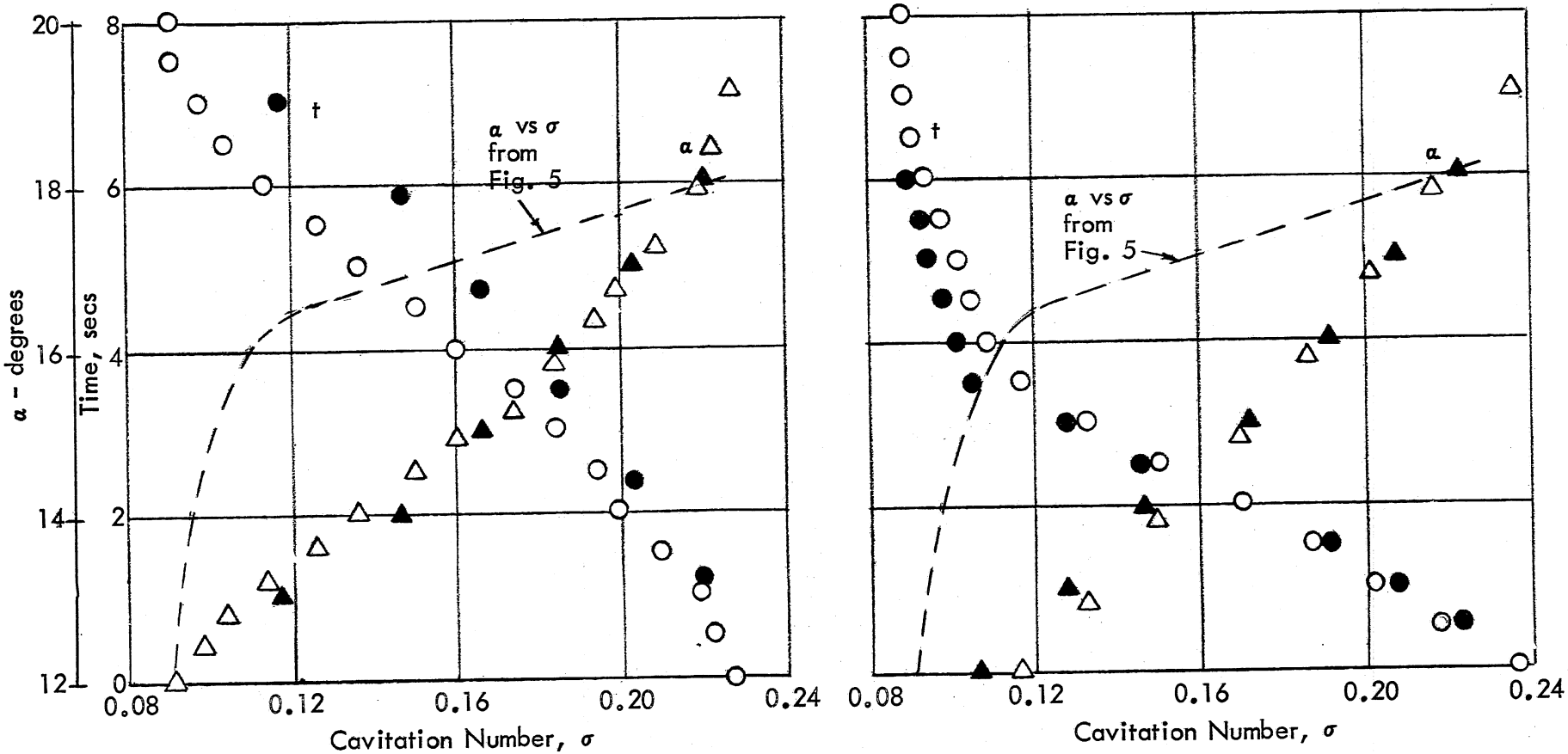

a) $\dot{\alpha} \approx -0.9$ deg/sec

b) $\dot{\alpha} \approx -2$ deg/sec

Fig. 8 - Change in Cavitation Number with Decreasing Angle of Attack, 19° to 12°

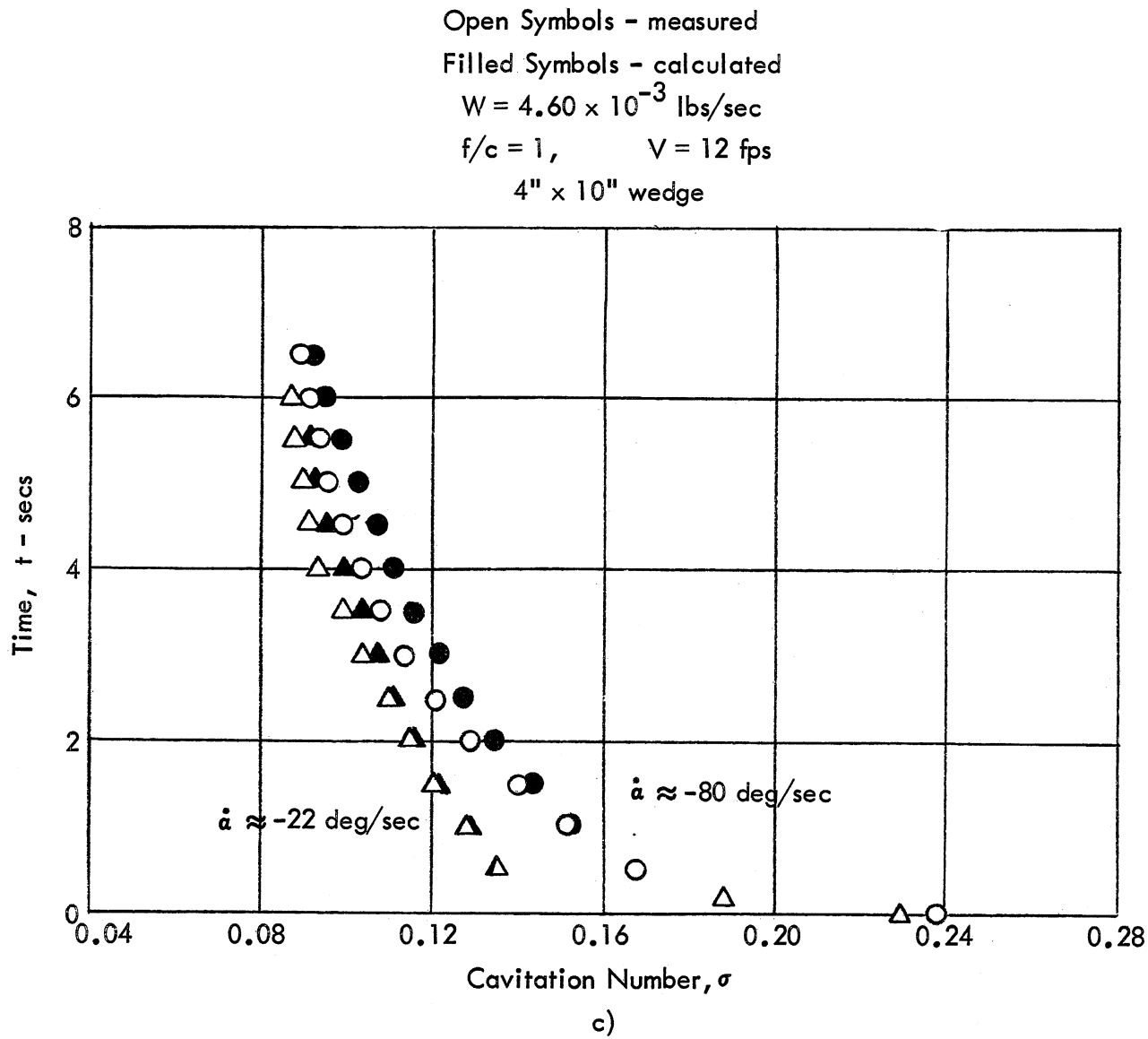

c)

Fig. 8 (contd.) - Change in Cavitation Number with Decreasing Angle of Attack, 19° to 12°

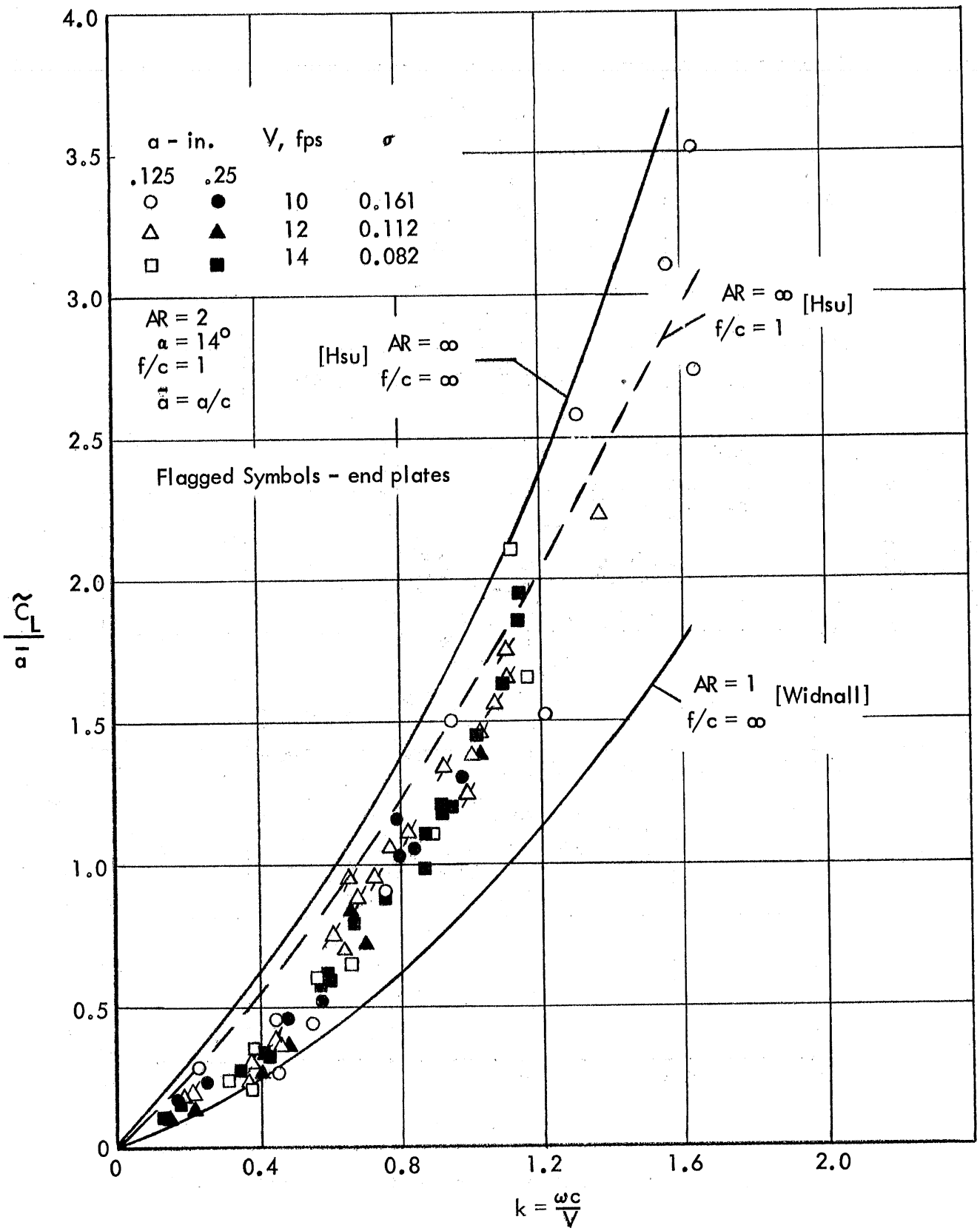

Fig. 9 - Amplitude of Oscillatory Lift Coefficient for Heaving Foil, AR = 2

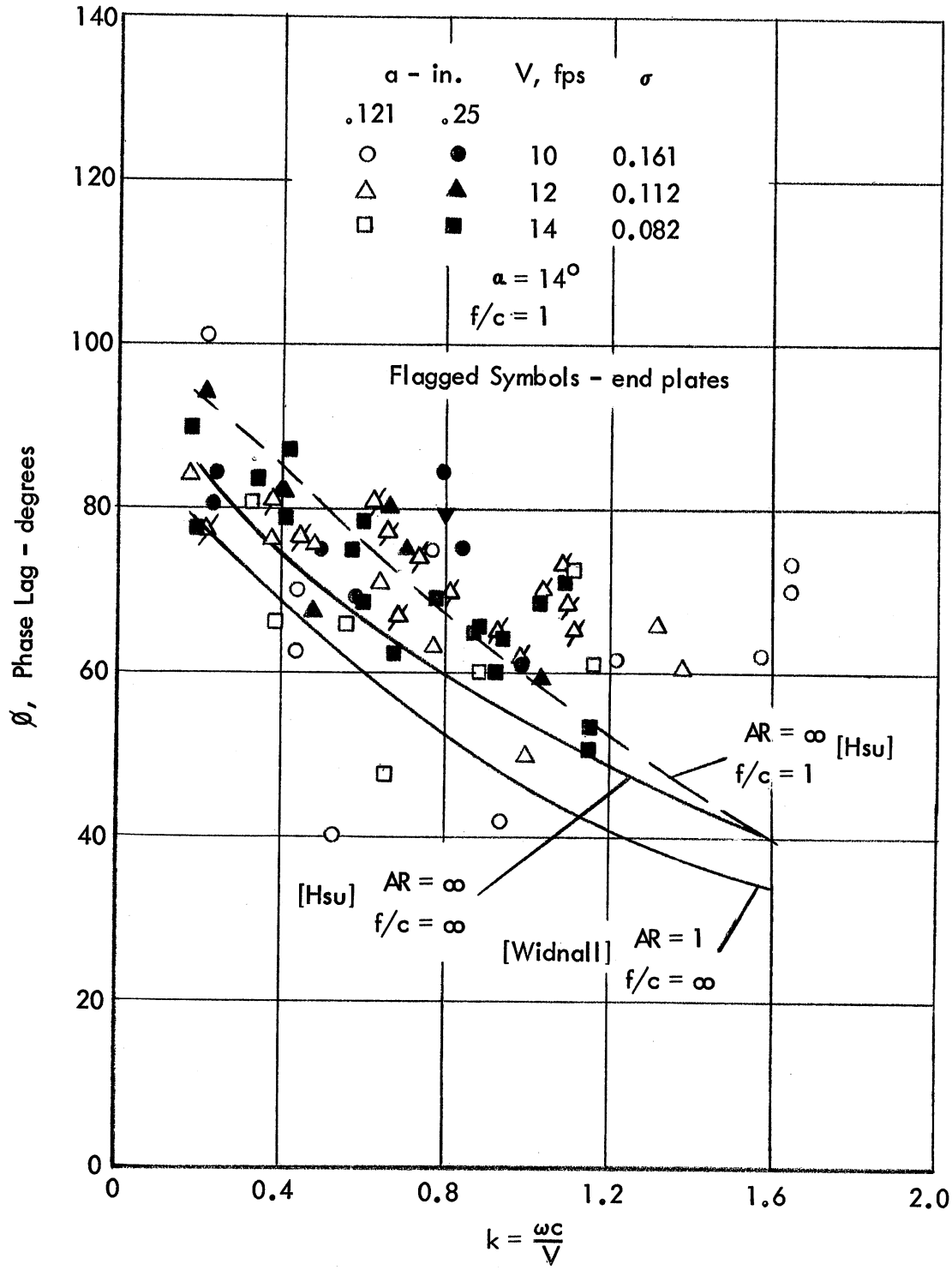

Fig. 10- Phase Lag of Oscillatory Lift Coefficient for Heaving Foil, AR = 2

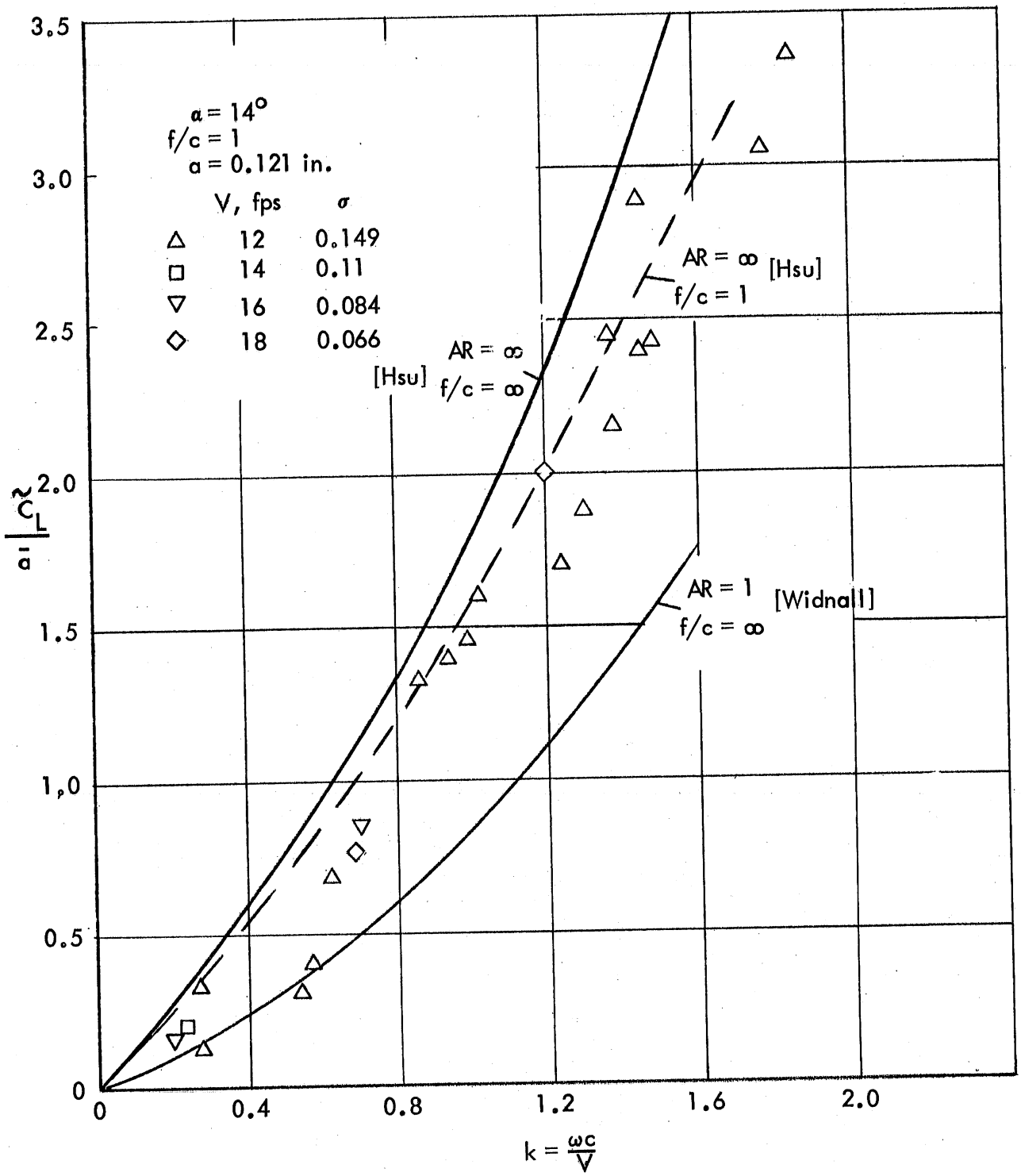

Fig.11 - Amplitude of Oscillatory Lift Coefficient for Heaving Foil, AR = 1

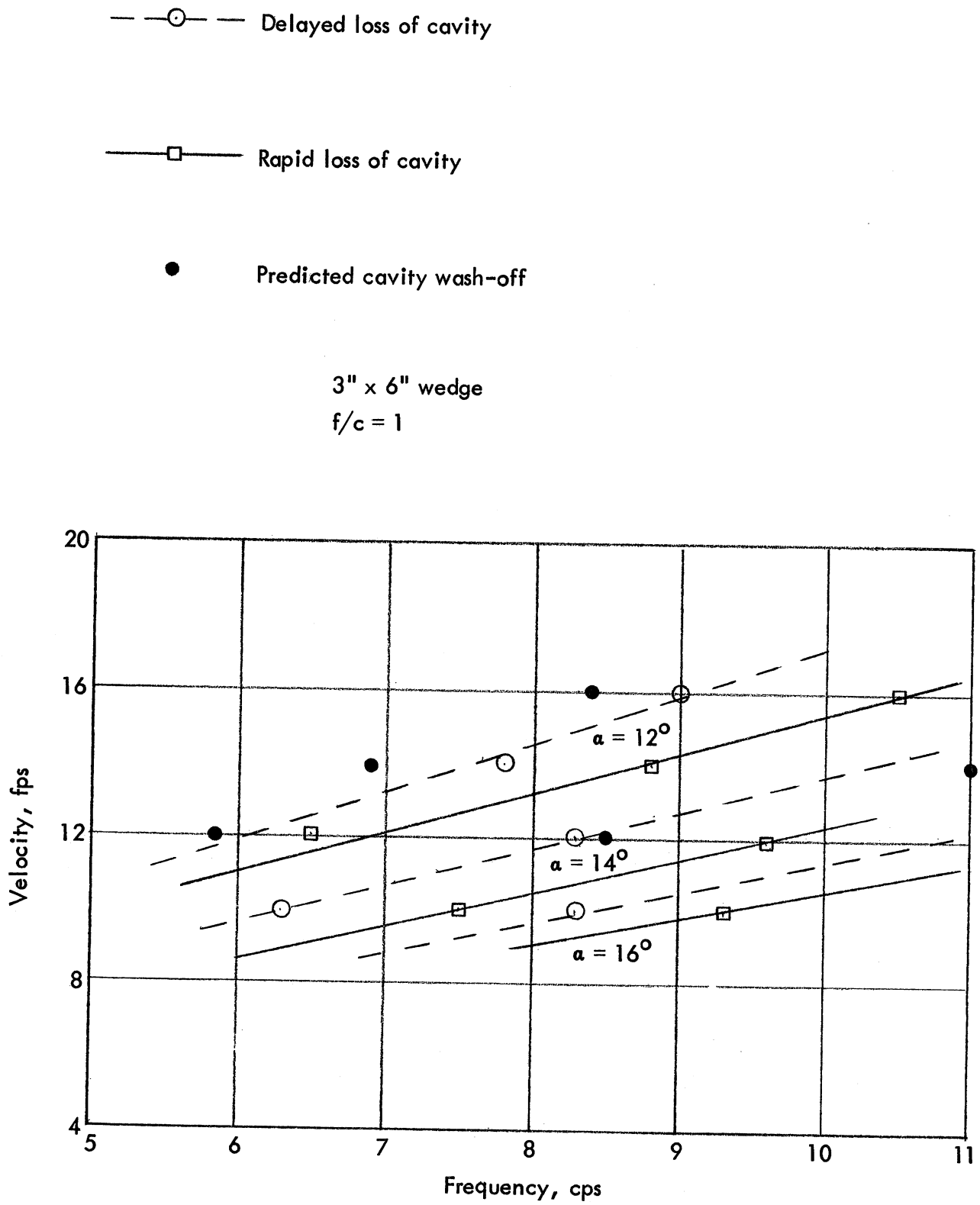

Fig. 12 - Cavity Wash-off During Heaving Oscillations, AR = 2

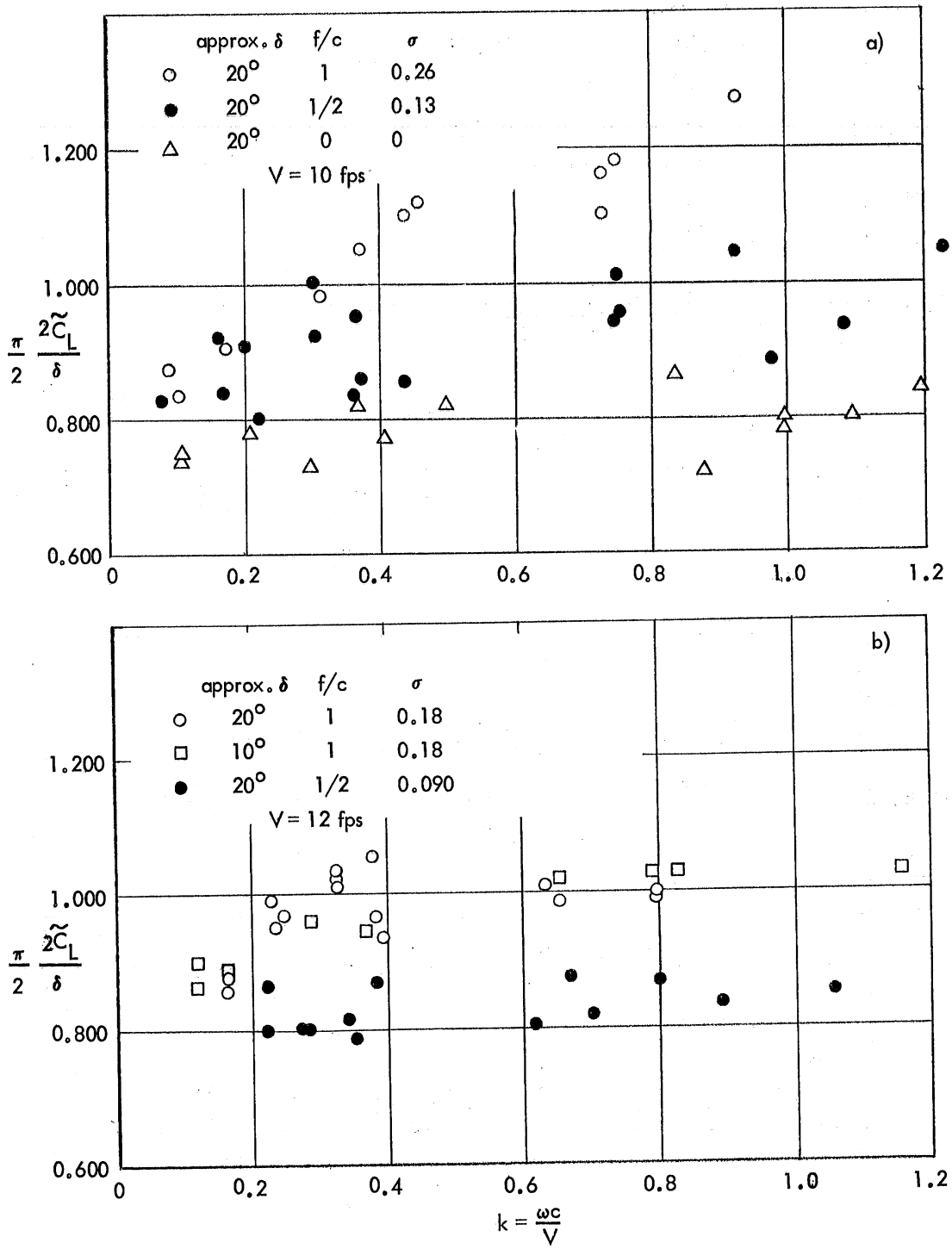

Fig. 13 - Amplitude of Oscillatory Lift Coefficient for Flapped Foil, AR = 2

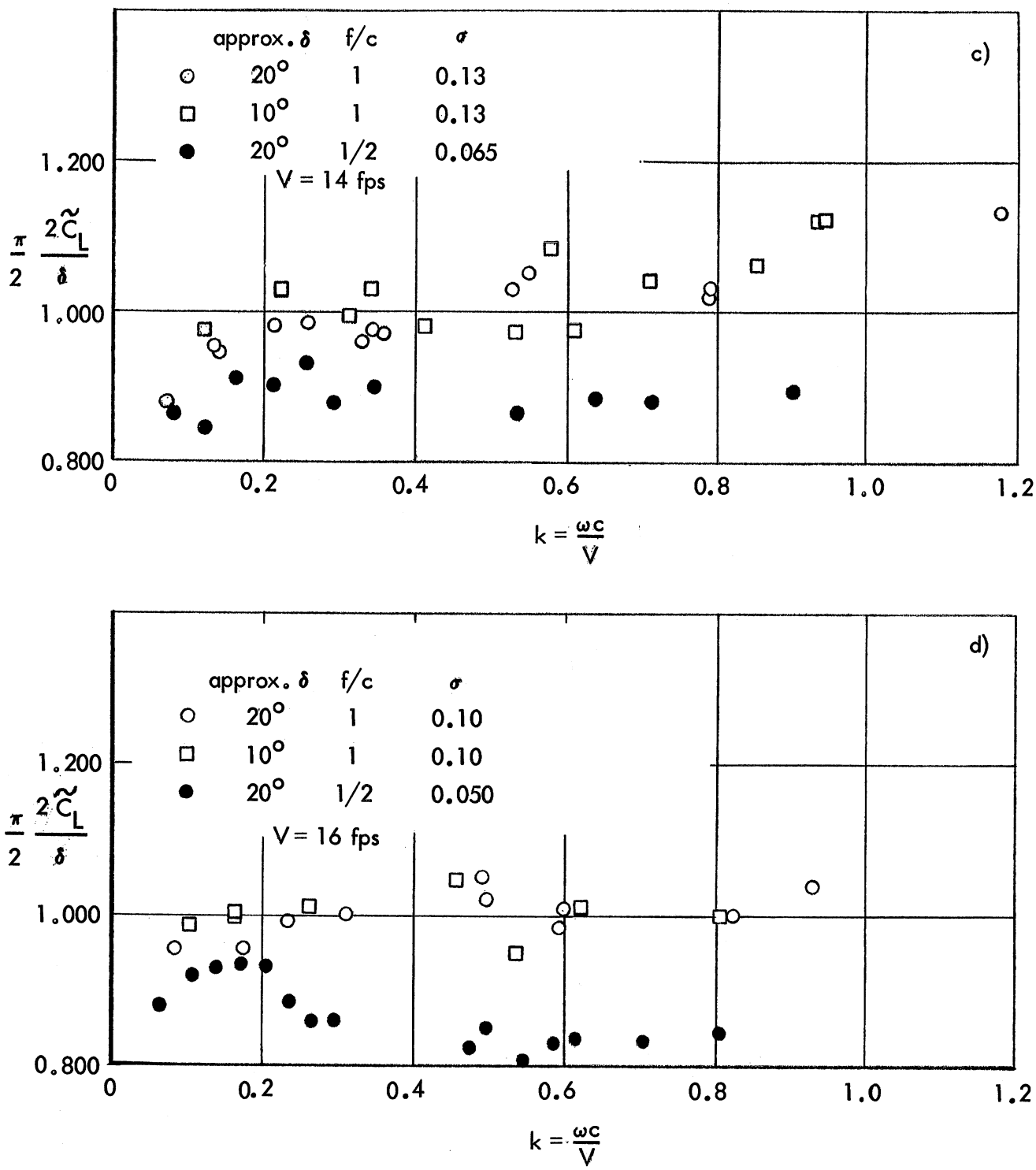

Fig. 13 (contd.) - Amplitude of Oscillatory Lift Coefficient for Flapped Foil, AR = 2

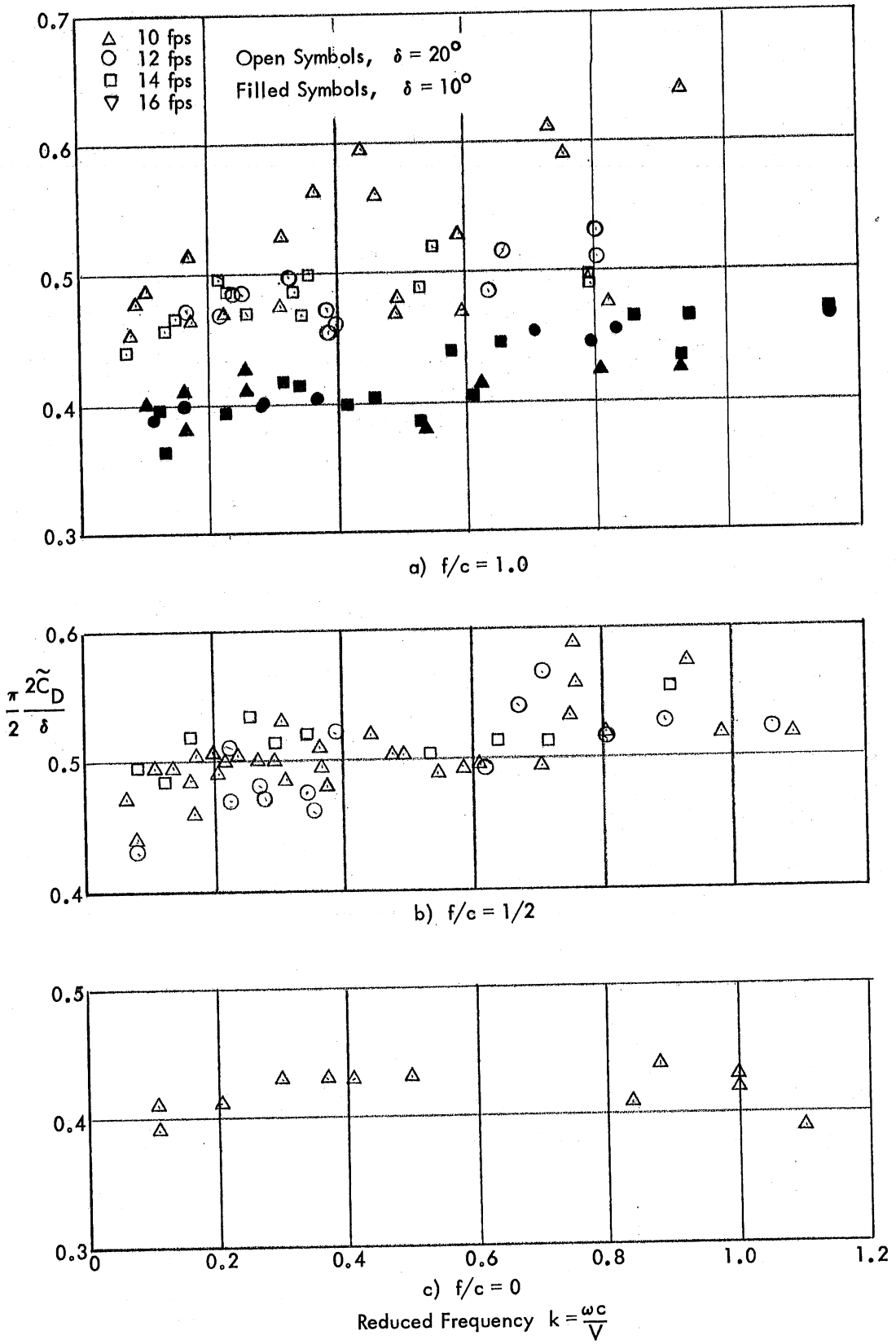

Fig. 14 - Amplitude of Oscillatory Drag Coefficient for Flapped Foil, AR = 2

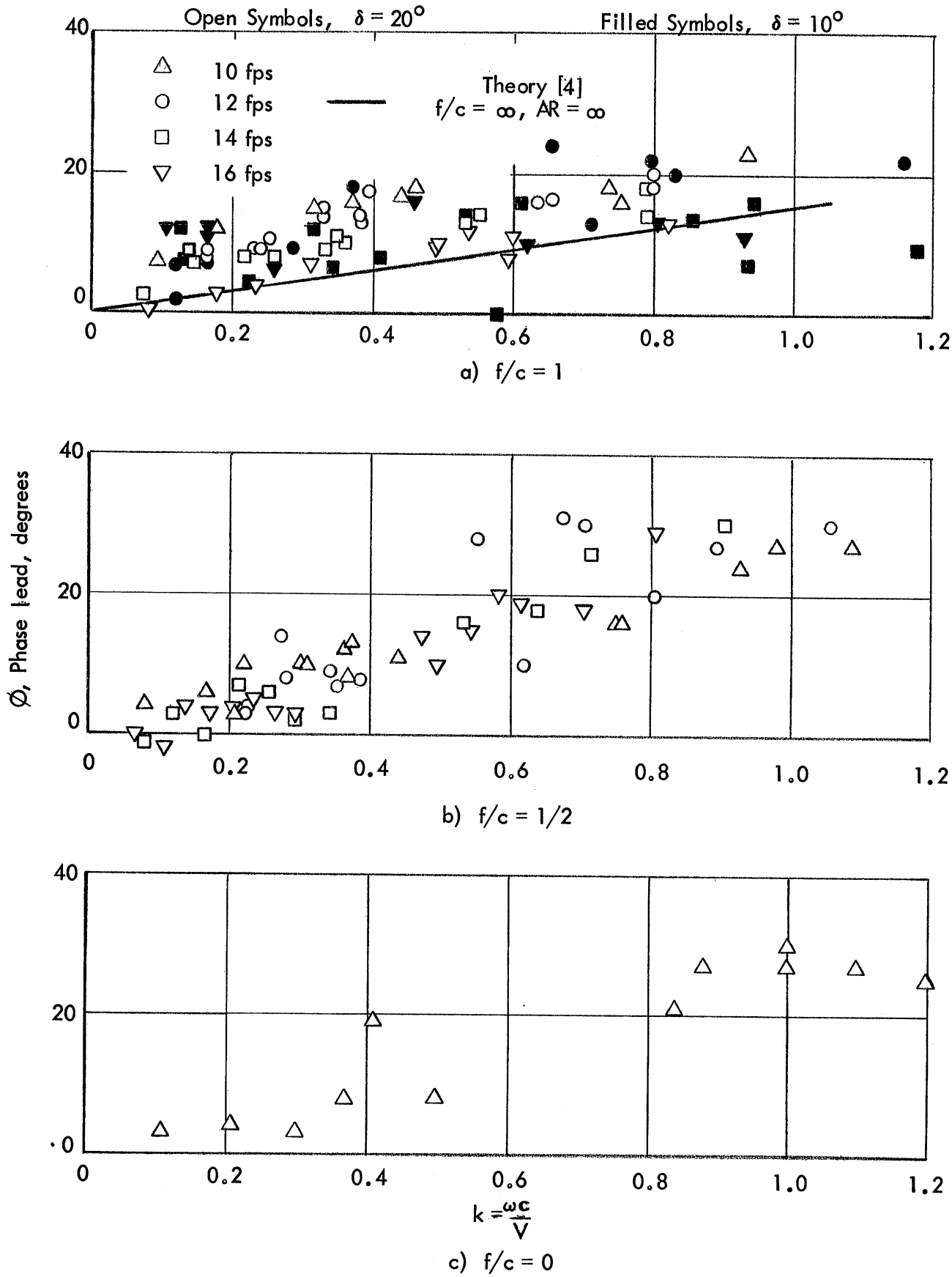

Fig. 15- Phase Lead of Oscillatory Lift Coefficient for Flapped Foil, AR = 2

DISTRIBUTION LIST FOR PROJECT REPORT NO. 85
of the St. Anthony Falls Hydraulic Laboratory

Copies	Organization
5	Chief of Naval Research, Department of the Navy, Washington, D. C., 20360, Attn: 3 - Code 438 1 - Code 461 1 - Code 463
1	Commanding Officer, Office of Naval Research Branch Office, 495 Summer Street, Boston, Massachusetts 02210.
1	Commanding Officer, Office of Naval Research Branch Office, 219 South Dearborn St., Chicago, Illinois 60604.
1	Office of Naval Research, New York Area Office, 207 W. 24th St., New York, New York 10011.
25	Commanding Officer, Office of Naval Research Branch Office, Box 39, FPO New York, New York 09510.
1	Commanding Officer, Office of Naval Research Branch Office, 1030 E. Green St., Pasadena, California 91101.
1	Office of Naval Research, San Francisco Area Office, 1076 Mission St., San Francisco, California 94103.
6	Director, U. S. Naval Research Laboratory, Washington, D. C. 20390, Attn: Code 2027.
15	Commanding Officer and Director, Naval Ship Research and Development Center, Washington, D. C. 20007, Attn: 1 - Code 042 1 - Code 500 1 - Code 513 1 - Code 520 1 - Code 521 1 - Code 525 1 - Code 526A 1 - Code 530 1 - Code 533 1 - Code 585 1 - J. L. Power (Code 589) 1 - Code 700 1 - Code 901 1 - Code 940 1 - Code 942
1	Commander, Naval Oceanographic Office, Washington, D. C. 20390.
1	Officer in Charge, Annapolis Division, Naval Ship Research and Development Center, Annapolis, Maryland 21402.

Copies	Organization
6	Commander, Naval Ship Systems Command, Department of the Navy, Washington, D. C. 20360, Attn: 1 - Code 0341 1 - Technical Library (Code 2021) 1 - Code 6305 1 - Code 6340 1 - Code 6440 1 - Code 6442
3	Commander, Naval Ordnance Systems Command, Washington, D. C. 20360, Attn: 1 - Code ORD 03 1 - Code ORD 05411 1 - Code ORD 913 (Library)
2	Commander, Naval Ship Engr. Center, Concept Design Division, Washington, D. C. 20360, Attn: 1 - Code 6110 1 - Code 6420
3	Maritime Administration, 441 G Street, N. W., Washington, D. C. 20235, Attn: 1 - Division of Engineering 1 - Office of Research and Development 1 - Division of Ship Design
1	Commander, Boston Naval Shipyard, Boston, Massachusetts 02129.
1	Commander, Charleston Naval Shipyard, U. S. Naval Base, Charleston, S. C. 29408.
1	Commander, Portsmouth Naval Shipyard, Portsmouth, New Hampshire 03801.
1	Commander, Norfolk Naval Shipyard, Portsmouth, Virginia 23709.
1	Commander (Code 246P), Pearl Harbor Naval Shipyard, Box 400, FPO San Francisco, California 96610.
1	Shipyard Technical Library, Code 130L7, Bldg. 746, San Francisco Bay Naval Shipyard, Vallejo, California 94592.
1	Commanding Officer and Director, Naval Applied Science Laboratory, Naval Base, Brooklyn, New York 11251, Attn: Code 930.
1	U. S. Naval Applied Science Laboratory, Technical Library, Building 1, Code 222, Flushing and Washington Aves., Brooklyn, New York 11251.
1	Mr. J. Z. Lichtman, Code 937, Naval Applied Science Lab., Brooklyn, New York 11251.

Copies	Organization
1	Commander, Naval Weapons Laboratory, Dahlgren, Virginia 22418, Attn: Technical Library.
1	Commander, Technical Lib. (Code 249b), Philadelphia Naval Shipyard, Philadelphia, Pennsylvania 19112.
1	Commanding Officer and Director, Navy Electronics Laboratory, San Diego, California 92152, Attn: Library.
1	Technical Library, Code H245C-3, Hunters Point Division, San Francisco Bay Naval Shipyard, San Francisco, California 94135.
4	Commander, Naval Ordnance Laboratory, White Oak, Silver Spring, Maryland 20910, Attn: 1 - Dr. A. May 1 - Chief, Lib. Div. 1 - Librarian 1 - Dr. R. E. Wilson, Assoc. Tech. Dir. (Aeroballistics)
1	Commander F, Naval Ordnance Laboratory, White Oak, Silver Spring, Maryland 20910.
1	Commanding Officer, Aberdeen Proving Ground, Maryland 21005, Attn: Tech. Lib. (Bldg) 313.
20	Defense Documentation Center, Cameron Station, Alexandria, Va. 22314.
1	Professor Bruce Johnson, Engineering Department, Naval Academy, Annapolis, Maryland 21402.
1	Superintendent, Naval Academy, Annapolis, Maryland 21402, Attn: Library.
1	Professor F. G. Hammitt, University of Michigan, Ann Arbor, Michigan 48108.
1	Dr. C. S. Yih, Department of Engineering Mechanics, University of Michigan, Ann Arbor, Michigan 48108.
1	Professor W. W. Willmarth, Department of Aero/Space Engineering, University of Michigan, Ann Arbor, Michigan 48104.
1	Dr. R. B. Couch, General Dynamics, Quincy Division, 97 E. Howard, Quincy, Mass. 02169.
1	AFOSR (SREM), 1400 Wilson Boulevard, Arlington, Va. 22209.
1	Dr. J. Menkes, Institute for Defense Analyses, 400 Army-Navy Drive, Arlington, Virginia 22204.
1	Library, Aerojet-General Corp., 6352 N. Irwindale Avenue, Azusa, California 91702.

Copies	Organization
5	University of California, Berkeley, California 94720, Attn: 1 - Librarian, Department of Naval Architecture 1 - Professor J. V. Wehausen, Department of Naval Architecture 1 - Professor P. Lieber 1 - Professor J. R. Paulling, Department of Naval Architecture 1 - Professor E. V. Laitone
2	Versuchsanstalt fur Wasserbau und Schiffbau, Schleuseninsel Im Tiergarten, Berlin, Germany, Attn: 1 - Dipl. Ing. A. Cross 1 - Professor Dr.-Ing. S. Schuster
3	Grumman Aircraft Eng. Corp., Bethpage, Long Island, N. Y. 11714, Attn: 1 - Mr. William P. Carl 1 - Mr. Robert Bower, Chief, Advanced Development 1 - Mr. Eugene F. Baird, Chief of Dynamic Analysis
1	School of Applied Mathematics, Indiana University, Bloomington, Indiana 47401.
1	Professor S. Siestrunck, Bureau d'Analyse de Recherches Appliquees, 6 Rice Louis Pasteur, 92 Boulogne, France.
1	Mr. F. Dell' Amico, Cornell Aeronautical Laboratory, Buffalo, New York 14221.
1	Dr. Irving C. Statler, Head, Applied Mechanics Department, Cornell Aeronautical Laboratory Inc., P. O. Box 235, Buffalo, New York 14204.
1	Mr. Richard P. White, Jr., Cornell Aeronautical Laboratory, 4455 Genessee Street, Buffalo, New York 14202.
1	Dr. Ronald Smelt, Vice President and Chief Scientist, Lockheed Aircraft Corporation, Burbank, California 91503.
1	Professor G. Birkhoff, Harvard University, Cambridge, Massachusetts 02138.
7	Massachusetts Institute of Technology, Cambridge, Massachusetts 02139, Attn: 1 - Professor H. Ashley, Room 33-408 1 - Professor M. Landahl, Room 33-406 1 - Professor M. A. Abkowitz, Dept. of Naval Architecture and Marine Engineering 1 - Professor P. Mandel, Room 5-325 1 - Professor R. F. Probstein, Department of Mechanical Eng. 1 - Professor A. T. Ippen 1 - Department of Naval Architecture and Marine Engineering, Room 5-228
1	Dr. W. J. Christian, Research Foundation, 10 West 35th Street, Chicago, Illinois 60616.

Copies	Organization
1	Mr. B. A. Napier, Vice Pres. and General Mgr., Lear Siegler, Inc., P. O. Box 6719, Cleveland, Ohio 44101.
1	NASA Lewis Research Center, 21000 Brookpark Road, Cleveland, Ohio 44135, Attn: Library MS 60-3.
1	NASA Scientific and Tech. Info. Fac., P. O. Box 33, College Park, Maryland 20740, Attn: Acquisitions Br (S-AK/DL).
1	Professor G. L. Von Eschen, Dept. of Aeronautical Astronautical Engineering, Ohio State University, Columbus, Ohio 43210.
1	Prof. Ir J. Gerritsma, Head Shipbuilding Lab., Tech. Univ., Mekelweg 2, Delft, The Netherlands.
1	Chrysler Corporation, Mgr. Advance Projects Organ., P. O. Box 1827, Detroit, Michigan 48231.
1	Ocean Systems, North American Aviation, Inc., 12214 Lakewood Blvd., Downey, California 90241.
1	C. A. Gongwer, Aerojet General Corporation, 9100 E. Flair Drive, El Monte, California 91734.
1	Baker Manufacturing Company, Evansville, Wisconsin 53536.
2	Northwestern University, Evanston, Illinois 60201. 1 - Professor Ali Bulent Cambel, Dept. of Mech. Eng. 1 - Professor A. Charnes, The Technological Institute
1	J. D. Malloy, President, Hydrosystems, Inc., 19 Engineers Lane, Farmingdale, New York 11735.
1	Dr. Martin H. Bloom, Polytechnic Institute of Brooklyn, Graduate Center, Dept. of Aerospace, Eng. and Applied Mechanics, Farmingdale, New York 11735.
1	Commanding General, Army Engineering R and D Labs., Tech. Documents Center, Fort Belvoir, Virginia 22060.
2	Colorado State University, Fort Collins, Colorado 80521, Attn: 1 - Professor Maurice L. Albertson, Prof. of Civil Engineering 1 - Prof. J. E. Cermak, Prof-in-Charge, Fluid Mechs. Pro.
1	Technical Library, Webb Institute of Naval Architecture, Glen Cove, Long Island, New York 11542.
1	Dr. H. Reichardt, Dir., Max Planck Institut fur Stromungsforchung, Bottingerstrasse 6-8, Gottingen, Germany.

Copies	Organization
2	Hamburgische Schiffbau-Versuchsanstalt, Bramfelder Strasse 164, Hamburg 33, Germany, Attn: 1 - Dr. H. W. Lerbs 1 - Dr. H. Schwaneche
2	Institute fur Schiffbau, University of Hamburg, Laemmersieth 90, 2 Hamburg 33, Germany, Attn: 1 - Professor G. P. Weinblum, Director 1 - Dr. K. Eggers
2	NASA, Langley Research Center, Langley Station, Hampton, Virginia 23365, Attn: 1 - Mr. D. J. Marten 1 - Library MS185
3	Stevens Institute of Technology, Davidson Laboratory, Hoboken, New Jersey 07030, Attn: 1 - Mr. J. P. Breslin 1 - Mr. D. Savitsky 1 - Mr. S. Tsakonas
2	Iowa Institute of Hydraulic Research, State University of Iowa, Iowa City, Iowa 52240, Attn: 1 - Prof. J. F. Kennedy, Director 1 - Professor L. Landweber
1	Library, Midwest Research Institute, 425 Volker Boulevard, Kansas City, Missouri 64110.
1	Professor John Miles, c/o I.G.P.P., University of California, San Diego, La Jolla, California 92038.
1	Dr. B. Sternlicht, Mechanical Technology Incorporated, 968 Albany-Shaker Road, Latham, New York 12110.
1	Mr. P. Eisenberg, President, Hydronautics Inc., Pindell School Rd., Howard County, Laurel, Maryland 20810.
1	Mr. Richard Barakat, Optics Department, Itek Corporation, Lexington, Massachusetts 02173.
1	Mr. Alfonso Alcedan L., Director, Laboratorio Nacional de Hydraulics, Antiguo Cameno A. Ancon, Casilla Postal 682, Lima, Peru.
1	Mr. C. Wigley, Flat 103, 6-9 Charterhouse Square, London E.C.1., England.
1	Professor A. F. Charwat, Department of Engineering, University of California, Los Angeles, California 90024.
1	Professor Carl Prohaska, Hydro-og Aerodynamisk Laboratorium, Lyngby, Denmark.

Copies	Organization
1	Dr. Jack Kotik, TRG, Incorporated, Route 110, Melville, New York 11746.
1	Dr. S. F. Hoerner, 148 Busteed Drive, Midland Park, New Jersey 07432.
4	St. Anthony Falls Hydraulic Laboratory, University of Minnesota, Mississippi River at 3rd Ave. S.E., Minneapolis, Minnesota 55414, Attn: 1 - Mr. J. M. Wetzel 1 - Professor C. E. Bowers 1 - Dr. C. S. Song 1 - Lorenz G. Straub Memorial Library
1	Superintendent, Naval Postgraduate School, Monterey, California 93940, Attn: Library.
1	Commanding Officer, USN Underwater Weapons and Research and Engineering Station, Newport, Rhode Island 02840, Attn: Technical Library.
2	Institute of Mathematical Sciences, New York University, 251 Mercer Street, New York, New York 10003, Attn: 1 - Professor A. Peters 1 - Professor J. J. Stoker
1	Engineering Societies Library, 345 East 47th Street, New York, N. Y. 10017.
1	Gibbs and Cox, Inc., Tech. Info. Control Section, 21 West Street, New York, New York 10006.
1	Society of Naval Architects and Marine Engineers, 74 Trinity Place, New York, New York 10006.
1	Professor A. G. Strandhagen, Department of Engineering Mechanics, University of Notre Dame, Notre Dame, Indiana 46556.
1	National Research Council, Aeronautical Library, Montreal Road, Ottawa 7, Canada, Attn: Miss O. M. Leach, Librarian.
1	Lockheed Missiles and Space Co., Technical Information Center, 3251 Hanover Street, Palo Alto, California 94301.
1	Officer in Charge, Naval Ordnance Test Station, Pasadena Annex, 3203 E. Foothill Blvd., Pasadena, California, Attn: Code P807.
4	California Institute of Technology, Pasadena, California 91109, Attn: 1 - Professor F. Zwicky, Department of Physics 1 - Professor T. Y. Wu 1 - Professor A. Acosta 1 - Dr. E. E. Sechler, Executive Officer for Aero

Copies	Organization
1	Professor R. C. MacCamy, Department of Mathematics, Carnegie Institute of Technology, Pittsburgh, Pennsylvania 15213.
2	Oceanics Inc., Technical Industrial Park, Plainview, Long Island, New York 11803, Attn: 1 - Dr. T. R. Goodman 1 - Dr. Paul Kaplan
1	Commander, Naval Missile Center, Point Mugu, California 93041.
1	Redstone Scientific Information Center, Army Missile Command, Redstone Arsenal, Alabama 35809, Attn: Chief, Document Section.
3	Southwest Research Institute, 8500 Culebra Road, San Antonio, Texas 78228, Attn: 1 - Mr. G. Ransleben 1 - Dr. H. N. Abramson 1 - Editor, Applied Mechanics Review
1	Professor W. R. Sears, 4927 Pacifica Drive, San Diego, California 92109.
2	General Dynamics Corp., Electric Boat Division, Marine Technology Center, P. O. Box 911, San Diego, California 92112, Attn: 1 - R. H. Oversmith, Mgr. Ocean Engr. 1 - W. B. Barkley
1	Convair Division of General Dynamics, P. O. Box 12009, San Diego, California 92112, Attn: Library (128-00).
1	Dr. Blaine R. Parkin, General Dynamics/Convair, P. O. Box 1128, Mail Zone 589-00, San Diego, California 92112.
1	Mr. G. Tedrew, Food Machinery Corporation, P. O. Box 367, San Jose, California 95103.
1	Library, The Rand Corp., 1700 Main St., Santa Monica, California 90401.
1	Mr. Schuyler Kleinhans, Vice President - Engineering, Douglas Aircraft Company, Inc., Santa Monica, California 90406.
1	Mr. Ross Hatte, Chief, Marine Performance Staff, The Boeing Co., Aero-Space Division, P. O. Box 3707, Seattle, Washington 98124.
1	Mr. Edwin U. Sowers, Prin. Engr., Bowles Engineering Corporation, 9347 Fraser Street, Silver Spring, Maryland 20910.
2	Department of Civil Engineering, Stanford University, Stanford, California 94305, Attn: 1 - Dr. Byrne Perry 1 - Professor E. Y. Hsu

Copies	Organization
1	Engineering Library, Dept. 218, Bldg. 101, McDonnel Aircraft Corp., P. O. Box 516, St. Louis, Missouri 63166.
1	Mr. Warren Bloomfield, Manager, Systems Engineering, Lycoming Division Avco Corporation, Stratford, Connecticut 06497.
1	Mr. R. W. Kermeen, Lockheed Missiles and Space Company, Department 57101, Bldg. 150, Sunnyvale, California 94086.
1	Mr. A. Silverleaf, National Physical Laboratory, Teddington, Middlesex, England.
1	Professor J. K. Lunde, Skipmodelltanken, Trondheim, Norway.
1	Professor J. Foa, Dept. of Aeronautical Engineering, Rennsselaer Polytechnic Institute, Troy, New York 12180.
1	Dr. M. Sevik, Ordnance Research Laboratory, Pennsylvania State University, University Park, Pa. 16801.
1	Library, The Marquardt Corporation, 16555 Saticoy, Van Nuys, California 91409.
1	Prof. Dr. Ir. J. D. Van Manen, Netherlands Ship Model Basin, Haagsteeg 2, Postbox 28, Wageningen, the Netherlands.
1	Science and Technology Div., Library of Congress, Washington, D. C. 20540.
1	National Academy of Sciences, National Research Council, 2101 Constitution Ave., N. W., Washington, D. C. 20360.
1	Defence Research and Dev. Attache, Australian Embassy, 1735 Eye Street N. W., Washington, D. C. 20006.
1	Librarian Station 5-2, Coast Guard Headquarters, 1300 E Street N. W., Washington, D. C. 20226.
1	Mr. T. A. Duncan, Lycoming Division, Avco Corporation, 1701 K Street N. W., Washington, D. C. 20002
1	Chief of Research and Development, Office of Chief of Staff, Department of the Army, The Pentagon, Washington, D. C. 20310.
1	Dr. Frank Lane, General Applied Science Lab, Merrick and Stewart Avenues, Westbury, Long Island, New York 11590.
1	Dr. F. W. Boggs, U. S. Rubber Company, Research Center, Wayne, New Jersey 07470.
1	Director, Woods Hole Oceanographic Institute, Woods Hole, Massachusetts 02543.

Copies	Organization
1	Dr. A. S. Iberall, President, General Technical Services, Inc., 8794 West Chester Pike, Upper Darby, Pennsylvania 19082.
1	Dr. H. Cohen, IBM Research Center, P. O. Box 218, Yorktown Heights, New York 10598.
1	Ir. W. Spuyman, Netherlands Ship Research Centre, Mekelweg 2, Delft, The Netherlands.
1	Professor Finn C. Michelsen, Naval Architecture and Marine Engr., 450 West Engineering Building, University of Michigan, Ann Arbor, Michigan 48108.
1	Professor Dr. L. van Wijngaarden, Technische Hogeschool Twente, Postbus 217, EMSCHEDE, The Netherlands.
1	Director, Scripps Institution of Oceanography, University of California, La Jolla, California 92037.
1	Director, Engineering Science Division, National Science Foundation, Washington, D. C. 20550.

Unclassified
Security Classification

DOCUMENT CONTROL DATA - R&D

(Security classification of title, body of abstract and indexing annotation must be entered when the overall report is classified)

1. ORIGINATING ACTIVITY *(Corporate author)* St. Anthony Falls Hydraulic Laboratory, University of Minnesota	2a. REPORT SECURITY CLASSIFICATION Unclassified 2b. GROUP

3. REPORT TITLE

UNSTEADY FORCE AND CAVITY CHARACTERISTICS FOR VENTILATED HYDROFOILS

4. DESCRIPTIVE NOTES *(Type of report and inclusive dates)*

Final Report

5. AUTHOR(S) *(Last name, first name, initial)*

Wetzel, J. M.
Foerster, K. E.

6. REPORT DATE	7a. TOTAL NO. OF PAGES	7b. NO. OF REFS
June 1967	38	7

8a. CONTRACT OR GRANT NO.	9a. ORIGINATOR'S REPORT NUMBER(S)
Nonr 710(48), Task NR 062-192 b. PROJECT NO. c. d.	Project Report No. 85 9b. OTHER REPORT NO(S) *(Any other numbers that may be assigned this report)*

10. AVAILABILITY/LIMITATION NOTICES

Distribution of this document is unlimited.

11. SUPPLEMENTARY NOTES	12. SPONSORING MILITARY ACTIVITY
	Office of Naval Research

13. ABSTRACT

Experimental measurements were made of the unsteady cavity and force characteristics for both forced and naturally ventilated hydrofoils of finite span submerged below a free surface. Unsteady cavity characteristics were studied for a force-ventilated wedge subjected to a sudden change in either the air flow rate to the cavity or angle of attack. Differences were observed in air entrainment rates measured for the unsteady case as compared to the corresponding instantaneous steady case. The magnitude of the differences depended on the kind of unsteadyness introduced.

Unsteady force characteristics were determined for naturally ventilated foils undergoing either a sinusoidal heaving motion or a harmonic oscillation of a trailing edge flap. The amplitude of the oscillatory lift was found to increase with increasing reduced frequency for a heaving foil, whereas the oscillatory lift was essentially constant up to reduced frequencies of 1.2 for the foil with an oscillating flap. There is limited agreement of the data with available theory.

DD FORM 1 JAN 64 1473 0101-807-6800

Unclassified
Security Classification

14. KEY WORDS	LINK A		LINK B		LINK C	
	ROLE	WT	ROLE	WT	ROLE	WT
Hydrofoils						
Ventilation						
Finite Span						
Unsteady Flow						

INSTRUCTIONS

1. ORIGINATING ACTIVITY: Enter the name and address of the contractor, subcontractor, grantee, Department of Defense activity or other organization *(corporate author)* issuing the report.

2*a*. REPORT SECURITY CLASSIFICATION: Enter the overall security classification of the report. Indicate whether "Restricted Data" is included. Marking is to be in accordance with appropriate security regulations.

2*b*. GROUP: Automatic downgrading is specified in DoD Directive 5200.10 and Armed Forces Industrial Manual. Enter the group number. Also, when applicable, show that optional markings have been used for Group 3 and Group 4 as authorized.

3. REPORT TITLE: Enter the complete report title in all capital letters. Titles in all cases should be unclassified. If a meaningful title cannot be selected without classification, show title classification in all capitals in parenthesis immediately following the title.

4. DESCRIPTIVE NOTES: If appropriate, enter the type of report, e.g., interim, progress, summary, annual, or final. Give the inclusive dates when a specific reporting period is covered.

5. AUTHOR(S): Enter the name(s) of author(s) as shown on or in the report. Enter last name, first name, middle initial. If military, show rank and branch of service. The name of the principal author is an absolute minimum requirement.

6. REPORT DATE: Enter the date of the report as day, month, year; or month, year. If more than one date appears on the report, use date of publication.

7*a*. TOTAL NUMBER OF PAGES: The total page count should follow normal pagination procedures, i.e., enter the number of pages containing information.

7*b*. NUMBER OF REFERENCES: Enter the total number of references cited in the report.

8*a*. CONTRACT OR GRANT NUMBER: If appropriate, enter the applicable number of the contract or grant under which the report was written.

8*b*, 8*c*, & 8*d*. PROJECT NUMBER: Enter the appropriate military department identification, such as project number, subproject number, system numbers, task number, etc.

9*a*. ORIGINATOR'S REPORT NUMBER(S): Enter the official report number by which the document will be identified and controlled by the originating activity. This number must be unique to this report.

9*b*. OTHER REPORT NUMBER(S): If the report has been assigned any other report numbers *(either by the originator or by the sponsor)*, also enter this number(s).

10. AVAILABILITY/LIMITATION NOTICES: Enter any limitations on further dissemination of the report, other than those imposed by security classification, using standard statements such as:

(1) "Qualified requesters may obtain copies of this report from DDC."

(2) "Foreign announcement and dissemination of this report by DDC is not authorized."

(3) "U. S. Government agencies may obtain copies of this report directly from DDC. Other qualified DDC users shall request through _____."

(4) "U. S. military agencies may obtain copies of this report directly from DDC. Other qualified users shall request through _____."

(5) "All distribution of this report is controlled. Qualified DDC users shall request through _____."

If the report has been furnished to the Office of Technical Services, Department of Commerce, for sale to the public, indicate this fact and enter the price, if known.

11. SUPPLEMENTARY NOTES: Use for additional explanatory notes.

12. SPONSORING MILITARY ACTIVITY: Enter the name of the departmental project office or laboratory sponsoring *(paying for)* the research and development. Include address.

13. ABSTRACT: Enter an abstract giving a brief and factual summary of the document indicative of the report, even though it may also appear elsewhere in the body of the technical report. If additional space is required, a continuation sheet shall be attached.

It is highly desirable that the abstract of classified reports be unclassified. Each paragraph of the abstract shall end with an indication of the military security classification of the information in the paragraph, represented as *(TS)*, *(S)*, *(C)*, *or (U)*.

There is no limitation on the length of the abstract. However, the suggested length is from 150 to 225 words.

14. KEY WORDS: Key words are technically meaningful terms or short phrases that characterize a report and may be used as index entries for cataloging the report. Key words must be selected so that no security classification is required. Identifiers, such as equipment model designation, trade name, military project code name, geographic location, may be used as key words but will be followed by an indication of technical context. The assignment of links, roles, and weights is optional.